







Review

# Technological and Operational Aspects That Limit Small Wind Turbines Performance

José Luis Torres-Madroño <sup>1</sup>, Joham Alvarez-Montoya <sup>1</sup>, Daniel Restrepo-Montoya <sup>1</sup>,  
Jorge Mario Tamayo-Avenidaño <sup>1</sup>, César Nieto-Londoño <sup>1,2,\*</sup> and Julián Sierra-Pérez <sup>1</sup>

<sup>1</sup> Grupo de Investigación en Ingeniería Aeroespacial, Universidad Pontificia Bolivariana, Medellín 050031, Colombia; jose.torresm@upb.edu.co (J.L.T.-M.); joham.alvarez@upb.edu.co (J.A.-M.); daniel.restrepomo@upb.edu.co (D.R.-M.); jorgemario.tamayo@upb.edu.co (J.M.T.-A.); julian.sierra@upb.edu.co (J.S.-P.)

<sup>2</sup> Grupo de Energía y Termodinámica, Universidad Pontificia Bolivariana, Medellín 050031, Colombia

\* Correspondence: cesar.nieto@upb.edu.co

Received: 19 October 2020; Accepted: 17 November 2020; Published: 22 November 2020



**Abstract:** Small Wind Turbines (SWTs) are promissory for distributed generation using renewable energy sources; however, their deployment in a broad sense requires to address topics related to their cost-efficiency. This paper aims to survey recent developments about SWTs holistically, focusing on multidisciplinary aspects such as wind resource assessment, rotor aerodynamics, rotor manufacturing, control systems, and hybrid micro-grid integration. Wind resource produces inputs for the rotor's aerodynamic design that, in turn, defines a blade shape that needs to be achieved by a manufacturing technique while ensuring structural integrity. A control system may account for the rotor's aerodynamic performance interacting with an ever-varying wind resource. At the end, the concept of integration with other renewable source is justified, according to the inherent variability of wind generation. Several commercially available SWTs are compared to study how some of the previously mentioned aspects impact performance and Cost of Electricity (CoE). Understanding these topics in the whole view may permit to identify both tendencies and unexplored topics to continue expanding SWTs market.

**Keywords:** small wind turbine; distributed generation; wind energy; aerodynamics; wind resource; manufacturing; control systems; hybrid systems; microgrid integration

## 1. Introduction

Energy demand augmented in 2018 above 2.3% according to the International Energy Agency, showing the fastest growth pace in the last decade [1,2]. Strategies conducted to supply such consumption must include a rapid increase in energy productivity, efficiency management strategies for energy systems, an integrated approach that uses centralized and decentralized sources, and a more significant share of renewable in the mix [3]. Depletion of fossil fuel sources and the associated effect of the non-rational use of this on the environment has raised the interest in searching alternatives accounting for the development, renovation, adaptation and even hybridization of different renewable [4–7] and non-renewable generation sources [8]. In this aim, the United Nations promotes the implementation of strategies conducting to ensure access to affordable, reliable, sustainable and modern energy for all [9].

It is worth to mention that hydropower facilities are important assets for the electric power sector and represent a key source of flexibility for electric grids with high penetrations of variable generation [10].

It is well known that hydropower dominance is the result of low energy costs and high hydro potential in countries where this resource is widely available. Nevertheless, the construction of large dams carries a significant environmental footprint because reservoirs modify the river's ecosystem [11]. Many in-service water resources and hydropower plants are in the aging stage, being sedimentation a significant issue in the watershed of reservoirs around the world [12], following the implementation of strategies for its management [13]. On the other hand, thermoelectric plants energy costs are dominated by fuel prices volatility, and at the same time, are a growing source of Greenhouse Gases despite some efforts to use alternative fuels [14], thermal energy storage [15] and waste heat recovery technologies [16,17] that provide valuable energy sources reducing the overall energy consumption.

Regarding the off-grid applications, 990 Small wind turbines (SWTs) were installed until 2015, representing 949 MW of installed capacity, achieving an increase of 5% in installed machines and 13% in installed capacity compared to 2014 [18]. In this sense, the installed capacity of SWTs represented 0.23% of the total installed capacity worldwide in 2015, showing the following composition: China with 43%, followed by the United States with 25%, and the UK and Italy with 15% and 6.3%, respectively [19]. During 2016 and 2017, a growth of 11% was observed corresponding to almost 53 MW in installed capacity. Until 2017, the off-grid systems served only 0.1% of the total wind energy installed capacity around the world [18,20]. Within SWTs installed capacity, the Horizontal-Axis Wind Turbine (HAWT) configuration has dominated the market over the last 30 years, where 74% of manufacturers focus their production on these models. Additionally, only one HAWT can achieve a higher average rated capacity than one Vertical-Axis Wind Turbine (VAWT). In this way, this review focused mainly on the pertinent issues that affect the performance of horizontal-axis SWTs and its potential impact on the CoE [18].

During 2018, in the United States alone, wind turbines of small and medium size accounted for 6.3% of the added capacity in distributed applications [21]. The 2019 worldwide wind power installed capacity rose to 622 GW, showing a market expansion of 19% with respect to 2018. Installed capacity increased by about 60 GW, approximately 10% more than in 2018 [22]. From the new capacity added at least more than 54 GW were onshore, of which, approximately 125.8 MW corresponded to SWTs installed capacity [23]; 6 GW were offshore, mainly represented in on-grid technologies as shown in Figure 1.

Actual SWTs are designed to operate at peak power output under relatively high wind speeds. From the wide variety of commercially available machines, a few examples from the smaller group of certified turbines have rated power at a wind speed of 11 m/s and peak power at 17, 12.6 and 16 m/s wind speed [24–26]. These examples correspond to typical three-bladed HAWTs (e.g., 80% of the small wind industry is dedicated exclusively to horizontal axis machines), which naturally can be expected to operate optimally at average power coefficients of around 0.45 and with a Tip Speed Ratio (TSR) of 6 to 7 approximately. Additionally, commercial wind turbines are targeted for sites with excellent wind resources, which reveals a gap in the remaining places, for which average wind speeds are well below 11 m/s.

Despite the growth in the use of SWTs to exploit low-speed wind resources, broad deployment of this technology still has technological and operational challenges to expand their implementation in rural and urban areas [27]. Regarding wind resource, SWTs operate in the lower part of the Atmospheric Boundary Layer (ABL) [28] or in low heights due to mechanical design and safety restrictions. Therefore, wind flow in these zones is not fully developed, presenting low-speed values when compare with completely-developed wind velocity profiles at greater heights. Compared with the implementation of SWTs in rural or open areas, its use in urban environments tends to be more complicated. As expected, the presence of turbulence and the vertical speed gradients, caused by the roughness of the terrain, reflects in an irregular behavior of the wind resource [29].

According to the foregoing, a successfully market penetration of SWTs requires the implementation of strategies that allow responding to the following challenges:

- Technology cost feasibility, in terms of manufacturing costs, maintenance costs and lifespan [30];
- Improvement in efficiency at low wind speeds in areas near the consumer centers where the resource may no be optimal [31];
- Noise control or reduction, owing to operation of SWTs is expected to be closer to the end-consumer, then turbines must be as quiet as possible [32]; and,
- Hybridization and integration with other sources of renewable energy, attending to the principle of spatial and temporal complementarity of the respective natural resources [33].

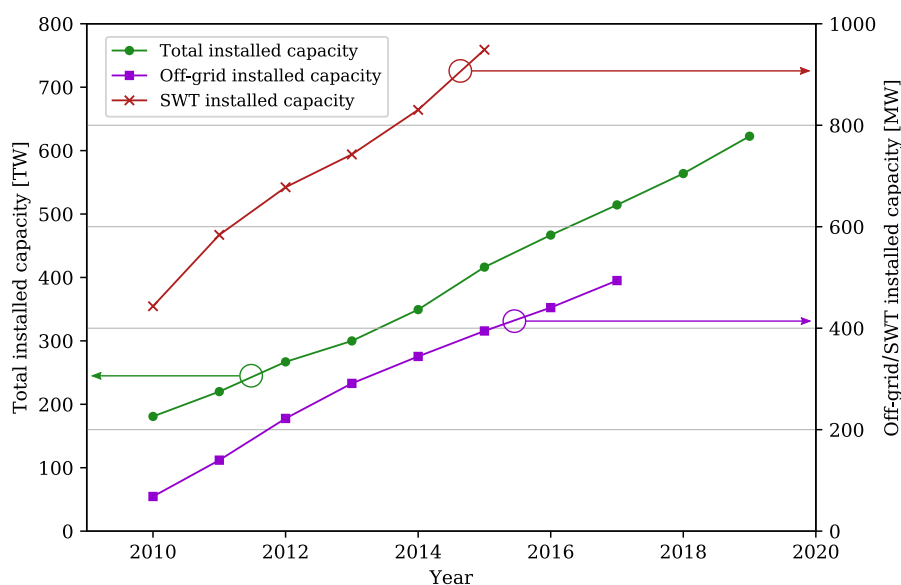


**Figure 1.** Cumulative installed capacity worldwide.

For all aforementioned challenges, arise the need to supply practical solutions in which SWTs can be used in low-wind speed environments (both rural or urban) with highly turbulent wind flows while being commercially affordable. In order to address these challenges, several multidisciplinary studies have been carried out in the last years in topics ranging from, but not limited to wind resource assessment, aerodynamics, manufacture, control systems or micro-grids integration. Among others, the following aspects stand out:

- As wind resource is the most differential factor when comparing SWTs with their large counterparts, most of the recent works have focused on it. Tadie Fogaing et al. [34] reviewed wind energy resources in urban locations, where is mentioned the requirement of SWT in applications close to consumption areas. Therefore, the wind energy study must have a precise evaluation of the wind speed profile.
- James and Bahaj [35] focused on micro- and small-scale wind turbine in the UK context. Principally, the authors addressed SWTs installed in buildings in the UK such as rural, suburban and urban environments. Additionally, the authors compared the wind speed computational tool called NOABL (Numerical Objective Analysis Boundary Layer) with annual measurements in rural, suburban and urban areas.
- Micallef and van Bussel [36] documented recent works related to SWTs and addressed a series of different disciplines connected to the aerodynamics in urban environments. The authors proposed an interesting discussion on the nature of existing methodologies for assessing wind resource in urban areas, encompassing analytical, experimental and numerical-based methods. KC et al. [37] presented a review on the topic of SWTs in the built environment aiming to understand issues related to wind resource, SWT performance, appropriate sitting and suitability of IEC 61400-2 in such environment.

- Within the context of rotor aerodynamic design, the work of Karthikeyan et al. [38] is one of the most relevant precedents, as they explore the self-starting behavior in SWTs, discuss on different devices for the improvement of performance and, gather information on airfoil sections for wind turbine blades for low Reynolds conditions, for which several design techniques are implemented.
- Regarding design control approaches, Menezes et al. [39] reviewed some relevant works related to the topic of wind turbine control divided into three main areas: wind turbine torque control, blade pitch control and grid integration control; it does not focus on SWTs neither vertical- nor horizontal axis-wind turbines. That works recognized the small number of works that address the wind turbine control concepts and presents a literature review of the topic to provide a base for further investigations in the field of wind turbine control techniques. In the discussion, the authors considered the potential of smart rotor applications and the overall potential of wind turbine control in the sustainable energy sector.

The previous analysis allows to conclude that most of the works reported regarding SWTs tend to focus on some specific issues without establishing a clear link between them, which would allow to have a more holistic view of the subject. In 2015, Tummala et al. [31] presented a review on SWTs discussing wind turbine classification, blade design, appropriate positioning, aero-acoustics, control and manufacturing in a holistic manner. However, its approach is mostly related to control without paying much attention to manufacturing issues. Although wind resource and aerodynamics are paramount in the effectiveness of energy harnessing by SWTs, the implementation of both, tailored manufacturing techniques and control systems, may contribute to further implementation of such machines.

Therefore, the aim of this paper is, on one hand, to provide a survey of the five main topics identified, i.e., wind resource, rotor aerodynamics, manufacture techniques, control systems and hybridization micro-grids of SWTs with horizontal-axis configuration. The interaction between these topics allows for a better understanding of the phenomenon in its whole and shows how one topic can be better understood when linked with the rest. On the other hand, a complement to the key topics of this review is provided by a comparative exercises between different commercially-available SWTs. This includes identifying the aspects mentioned previously under different resources and operating conditions and the respective effect on the performance and finally the impact on the CoE. This procedure is structured around six different wind turbine models, each one with particular characteristics of performance and manufacturing that illustrate the diversity evidenced in survey sections.

The comprehensive analysis of the wind resource (Section 2) and the effects of turbulence over SWTs operation (Section 3) produces a fundamental input for the decisions over the aerodynamic design of the wind turbine rotor (Section 4). The final shape of the blades is a key factor for the selection of the required manufacturing technique that guarantees both the aerodynamic shape of the blades and their structural integrity as illustrated in Section 5. In addition, the blades' control system (Section 6) would have to account for the aerodynamic performance of the blades and its interaction with the available wind resource. The above wind turbine topics affect the integration of SWTs with other renewable sources, driving the research studies to hybrid micro-grid design to improve the energy security of some regions. (Section 7). The identified topics and their interactions are shown in Figure 2. Finally, the assessment of commercial wind turbines and the effect of the aforementioned topics over its performance and the CoE is presented in Section 8.

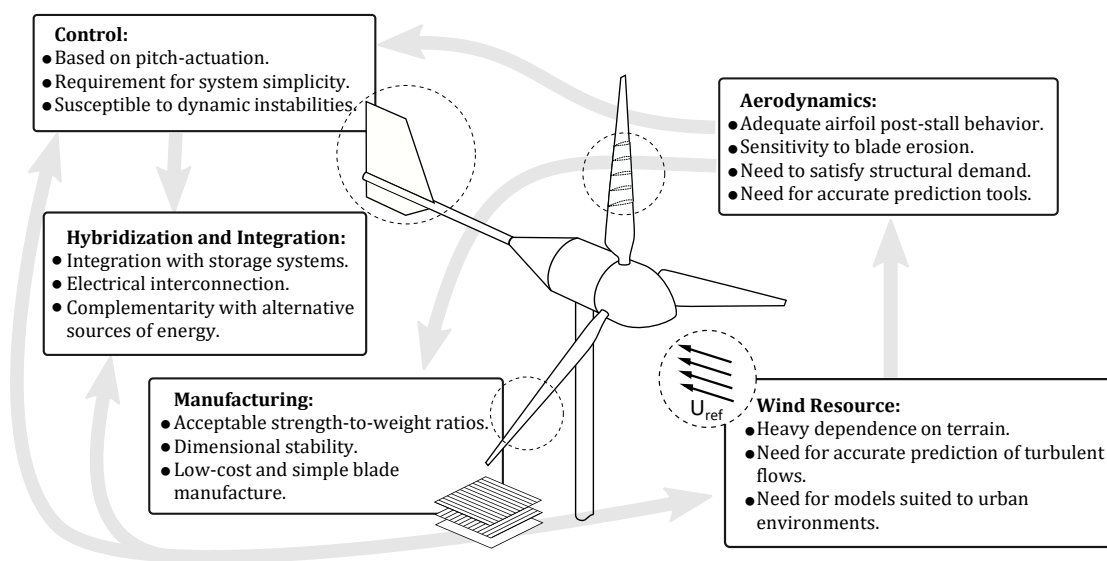


Figure 2. Interaction of the proposed topics for the review.

## 2. Wind Resource Estimation

Global Wind Power Potential (WPP) has been estimated in 94.5 TW; regions with the highest WPP are Europe, Russia, and the United States with 37.5, 36 and 11 TW, respectively [40]. However, data from the European Wind Energy Association shows that low-speed winds are the most frequent; around 14 % of the time, the wind is too slow to produce electricity with large scale wind turbines [41].

More recently, projections of the wind energy resource for most of the coastal region of the United States shows a steady decrease, which would compromise the capacity to fully exploit the region's total WPP with offshore large-scale wind turbines [42]. Among that, the lack of exact predictability and fluctuations of wind energy, conduces to problems in the power flow of transmission system, especially when the weak nature of the grid in remote areas and the uncertainty of wind are taken into consideration [43].

Deployment of SWTs commonly includes its installation and operation in rural areas and urban environments. An appropriate estimation and assessment of the wind resources, including wind velocity distribution and variation over time, is mandatory to determine the power generation and load distribution on wind turbine's components. In this sense, this section reviews the models to evaluate wind speed, including those defined within the IEC standard to evaluate wind profiles in open terrains for pre-feasibility of SWTs projects. Finally, some studies related to the behavior of small wind turbines in urban areas are presented.

### 2.1. Wind Speed Estimation

Wind speed, from a mathematical point of view, is represented by space and time variables. If the analysis is independent of time, the model usually employed to determine the wind profile developed on a surface is described by the logarithmic law, as [36,44]:

$$u_{\infty}(y) = \frac{u_*}{\kappa} \ln \left( \frac{y-d}{y_0} \right), \quad (1)$$

where  $u_{\infty}(y)$  is the wind speed depending on the height above ground level  $y$ ,  $\kappa$  is the von Karman constant,  $d$  is the zero-plane displacement where the wind speed has a value of 0 m/s,  $y_0$  is the roughness

height given by the aerodynamic effects of surface imperfections (typical values are given in Table 1), and  $u_*$  is the friction velocity due to the ground surface given as:

$$u_*^2 = \frac{\tau_w}{\rho}, \quad (2)$$

where  $\rho$  is the air density and  $\tau_w$  is the wall shear stress [45].

**Table 1.** Values of height of roughness for some terrain types [36].

Terrain Type	$y_0$
Cities, forests	0.7
Suburbs, wooded countryside	0.3
Villages, country with trees	0.1
Open farmland, few trees and buildings	0.03
Flat grassy planes	0.01
Flat desert, rough seas	0.01

Wind speed anemometer measurements  $u_{ref}$  are used as reference values at the evaluation height  $y_{ref}$  to determine the speed magnitude for any other height  $y$  given by [46,47]:

$$u_\infty(y) = u_{ref} \left( \frac{y}{y_{ref}} \right)^\alpha, \quad y < y_{ref}, \quad (3)$$

being  $\alpha$  the roughness coefficient of the ground. For a preliminary analysis, the values shown in the Table 2 can be used [47].

**Table 2.** Values of roughness coefficient  $\alpha$  for some terrain types [47].

Terrain Type	$\alpha$
Calm sea	0.09
Agricultural area—limited presence of obstacles less than 6 m high	0.12
Agricultural area—limited presence of obstacles between 6 m and 8 m high	0.16
Agricultural area—a lot of presence of obstacles between 6 m and 8 m high	0.20
Urban or forest area	0.30

On the other hand, the wind speed profile have variable behavior respect to the time. The statistical models are an alternative to describe the stochastic behavior of wind magnitude and direction [48]. In this regard, the Weibull and Rayleigh are Probability Distribution Functions (PDF) commonly used to characterize wind speed magnitude frequency. Additionally, these models are usually used to estimate the Annual Energy Production (AEP) [36]. The Weibull function is given by:

$$W(u_\infty) = \left( \frac{k}{c} \right) \left( \frac{u_\infty}{c} \right)^{k-1} \exp \left[ - \left( \frac{u_\infty}{c} \right)^k \right], \quad (4)$$

where  $k$  is the function shape parameter, and  $c$  is a scale parameter [36,40]. In the literature, the shape parameter is related to the terrain morphology and the wind regime, where some typical values are reported in Table 3 [47], given the scale parameter as [49,50]:

$$c = \frac{u_{mean}}{\Gamma(1 + \frac{1}{k})}, \quad (5)$$



where,  $u_{mean}$  is the mean wind speed, and  $\Gamma$  is the gamma function. Rayleigh distribution is a case where the Weibull model takes the scale parameter  $c$  equal to two (2) [40] and it is given by IEC standard [51] as:

$$R(u_{hub}) = 1 - \exp \left[ -\pi (u_{hub}/2u_{ave})^2 \right], \quad (6)$$

being  $u_{hub}$  the average wind speed at the height of the wind turbine rotor over 10 min, and  $u_{ave}$  the annual average wind speed at the same height of  $u_{hub}$  [51]. Finally, the annual energy production by Weibull PDF is calculated as:

$$AEP = T \int_{u_{in}}^{u_{out}} W(u_{\infty}) P(u_{\infty}) du_{\infty}, \quad (7)$$

where  $AEP$  refers to the total energy generated over time operation  $T$ ,  $u_{in}$  is the cut-in wind speed,  $u_{out}$  is the cut-out wind speed,  $P(u_{\infty})$  is the power output given by the characteristic curve of the specific wind turbine to be evaluated [36], and  $W(u_{\infty})$  is the Weibull distribution given by Equation (4).

The statistical approaches are usually adjusted by real density values of air at the installation place and corrected due to changes in pressure or temperature. It is also modified by system performance, in terms of maintenance or availability of the power grid. The main disadvantage of this approach is that is based on statistical models of wind measurements and the manufacturer's  $P$ - $V$  curve (i.e., generation power as a function of wind speed). These values are usually experimentally estimated in a wind tunnel with controlled parameters [29], being somehow not enough accurate when compared with the case of real conditions.

**Table 3.** Values of shape parameter  $k$  for some terrain types [36].

Terrain Morphology	$k$
Mountainous area	1.2–1.7
Great plains—Hills	1.8–2.5
Open area	2.5–3.0
coastal zone	3.1–3.5
Islands	3.5–4.0

## 2.2. CFD Wind Velocity Profile Estimation

The evaluation of potential SWT sites begins by recognizing the wind resource; random, erratic, and uncontrollable behavior [52] present in large wind farms or rural areas gets worse due to buildings' presence. Among others, turbulence high levels add constant changes in magnitude and direction of the wind speed affecting wind energy harnessing and reliability. Due to this, the prediction of the wind profile by Computational Fluid Dynamics (CFD) stands out for its comprehensive implementation [36,52,53].

The Unsteady Reynolds-Averaged Navier-Stokes (URANS) represents the conservation of mass and momentum for incompressible fluids without body forces [53–55]. This model is commonly used for wind resources characterization; it is formed by the continuity equation given by [56]:

$$\frac{\partial \bar{u}_i}{\partial x} = 0, \quad (8)$$

and the conservation of the momentum:

$$\frac{\partial \bar{u}_i}{\partial t} + \frac{\partial}{\partial x_j} (\bar{u}_i \bar{u}_j) = -\frac{1}{\rho} \frac{\partial \bar{p}}{\partial x_i} + \nu \frac{\partial^2 \bar{u}_i}{\partial x_j \partial x_j} - \frac{\partial}{\partial x_j} (\overline{u'_i u'_j}), \quad (9)$$

where  $\bar{u}_i$  denotes the mean velocity,  $u'_i$  is the fluctuation velocity,  $\nu$  is the kinematic viscosity, and  $\overline{u'_i u'_j}$  is the Reynolds-stress tensor, which is an unknown variable, that is possible to solve using Boussinesq eddy-viscosity assumption [56,57] given by the following expressions:

$$\tau_{ij} = \overline{u'_i u'_j} = \frac{2}{3} k \delta_{ij} - \nu_t \left( \frac{\partial \bar{u}_i}{\partial x_j} + \frac{\partial \bar{u}_j}{\partial x_i} \right), \quad (10)$$

$$k = \frac{1}{2} \overline{u'_i u'_i} = \frac{1}{2} \left( \overline{u_1^2} + \overline{u_2^2} + \overline{u_3^2} \right), \quad (11)$$

where  $k$  is the turbulent kinetic energy and  $\nu_t$  is the kinematic eddy viscosity [58]. Additionally, it is necessary to find two turbulence properties [56], the turbulent kinetic energy  $k$  and the turbulent dissipation rate  $\varepsilon$  given by the equations:

$$\frac{\partial k}{\partial t} + \bar{u}_j \frac{\partial k}{\partial x_j} = \frac{\partial}{\partial x_j} \left[ \frac{(v + \nu_t)}{\sigma_k} \frac{\partial k}{\partial x_j} \right] - \varepsilon + \tau_{ij} \frac{\partial \bar{u}_i}{\partial x_j}, \quad (12)$$

$$\frac{\partial \varepsilon}{\partial t} + \bar{u}_j \frac{\partial \varepsilon}{\partial x_j} = \frac{\partial}{\partial x_j} \left[ \frac{(v + \nu_t)}{\sigma_\varepsilon} \frac{\partial \varepsilon}{\partial x_j} \right] + C_{\varepsilon 1} \frac{\varepsilon}{k} \tau_{ij} \frac{\partial \bar{u}_i}{\partial x_j} - C_{\varepsilon 2} \frac{\varepsilon^2}{k}, \quad (13)$$

where  $\nu_t$  is given by [56]:

$$\nu_t = C_\mu \frac{k^2}{\varepsilon}, \quad (14)$$

and  $\sigma_k$  and  $\sigma_\varepsilon$  are Prandtl numbers, and  $C_{\varepsilon 1}$ ,  $C_{\varepsilon 2}$  and  $C_\mu$  are model constant [54,55,59]. The above CFD formulation is known as the Standard  $k - \varepsilon$  model (SKE). Alternative approaches for reproducing rural and urban wind conditions include variations of the SKE formulation [54], Reynolds Stress Models (RSM) or Large-Eddy Simulation (LES) techniques [53].

### 2.3. Standard IEC 61400-2

The IEC 61400-2 is the international regulation for SWT. This standard defines four site classes in terms of wind speed and turbulent effects, which are a characteristic of the zone and differ depending on the application site are shown in Table 4, where  $I_{15}$  is the characteristic value of the turbulence intensity at a wind speed of 15 m/s and  $a$  is a dimensionless adjustment parameter; it is worth to mention that these classes should not be considered for off-shore applications or when the environment presents tropical storms [51].

**Table 4.** Application Site Classes for Small Wind Turbines given by IEC 61400-2 Standard [51].

SWT Class	I	II	III	IV
$u_{ref}$ [m/s]	50	42.5	37.5	30
$u_{ave}$ [m/s]	10	8.5	7.5	6
$I_{15}$	0.18	0.18	0.18	0.18
$a$	2	2	2	2

The standard defines two wind regimes: Normal Wind Speed Conditions (NWC) and Extreme Wind Speed Conditions (EWC). The wind regimes and the SWT class depicted in Table 4 define the Standard Wind Speed Conditions (SWC). SWTs designs under the NWC regime take into account the Rayleigh distribution (see Equation (6)) according to the IEC standard [51]. Furthermore, the NWC regime also determines the Normal Wind Speed Profile (NWP)  $u_\infty(y)$  (see Equation (3)) [46,51], with a value of  $\alpha$  of



0.2. The last NWC factor is the Normal Turbulence Model (NTM); it describes the stochastic fluctuation of wind speed according to 10 min average measurements including the effect of magnitude and wind speed direction variation [51].

On the other hand, to account for extreme wind loads, the IEC standard suggests the EWC regime, which includes peak wind speed and sudden changes in direction among others. The Extreme Wind Speed Model (EWM) addresses the 3-second gust speed estimated to be exceeded on the average only once in 50 years given by:

$$u_{e50}(y) = GF u_{\text{ref}} (y/y_{\text{hub}})^{0.11}, \quad (15)$$

as well, the one expected in one year is [51]:

$$u_{e1} = 0.75 u_{e50}. \quad (16)$$

In Equations (15) and (16),  $y_{\text{hub}}$  refers to the hub height of the wind turbine, and  $GF$  is the gust factor defined by the IEC standard as 1.4. Both equations take into account the average variation of the wind direction within  $-15^\circ$  and  $15^\circ$  [60]. Specifically,  $GF$  is given as [61]:

$$GF = \frac{\hat{u}_\infty}{\bar{u}_\infty}, \quad (17)$$

where  $\hat{u}_\infty$  is a wind speed peak or gust and  $\bar{u}_\infty$  refers to the average wind speed. The American Society of Civil Engineers Standard establishes that a 3-s gust duration is sufficient to perceive structural damage. Following the IEC standard, a  $GF$  of 1.4 ensures that a SWT under the corresponding reference wind speed, will be safe under 3-second gusts; for these cases, the reference wind speed refers to 10 min average measurements [62].

The  $GF$  model is simple but it does not represent the real gust profile [60]. Into the EWC regime, the Extreme Operating Gust (EOG) stands that gust magnitude over  $N$  years at the hub height is [51]:

$$u_{\text{gust},N} = \beta \left( \frac{\sigma_1}{1 + 0.1 \left( \frac{D}{\Lambda_1} \right)} \right), \quad (18)$$

where  $D$  is the rotor diameter,  $\beta$  takes values of 4.8 and 6.4 for periods of one ( $N = 1$ ) and 50 years ( $N = 50$ ), respectively; on the other side,  $\Lambda_1$  is the turbulence scale parameter given by:

$$\Lambda_1 = \begin{cases} 0.7 \text{ m} * y_{\text{hub}} & \text{for } y_{\text{hub}} < 30 \text{ m}, \\ 21 \text{ m} & \text{for } y_{\text{hub}} \geq 30 \text{ m}, \end{cases} \quad (19)$$

and, being  $\sigma_1$  the standard deviation of the longitudinal velocity component expressed as [51]:

$$\sigma_1 = I_{15} (15 + a u_{\text{hub}}) / (a + 1). \quad (20)$$

Finally, the EWC defines the Extreme Direction Change (EDC) by means of:

$$\theta_{eN}(t) = \pm \beta \arctan \left( \frac{\sigma_1}{u_{\text{hub}} \left( 1 + 0.1 \left( \frac{D}{\Lambda_1} \right) \right)} \right). \quad (21)$$

which is defined over the same periods described by EOG, where  $\beta$  takes the same values defined for Equation (18) [51].

### 3. Turbulence Effects on Wind Profiles and STWs Performance

The IEC 61400-2 standard models are applicable for open terrain wind measurements; however, its use for urban environments required considering obstacles and surface roughness present in operation areas. Urban environments have more turbulent intensity effects than open terrains. The impact of turbulence in the wind generation system is considered during the SWTs design process; if not, power generation estimation will not be correct and structural components may fail during the operation [63]. Some works that present cases in which the SWTs are evaluated under the cited standard are listed below.

The Turbulence Intensity  $TI$  is commonly used to evaluate the effect of turbulence effect over SWTs operation and is given by [64]:

$$TI = \frac{\sigma_{u_{\infty}}}{\bar{u}_{\infty}}, \quad (22)$$

where  $\sigma_{u_{\infty}}$  is the standard deviation of wind speed measurements over 10 min and  $\bar{u}_{\infty}$  is the average wind speed over the same time interval [64]. It is worth to mention that the turbulence intensity does not include a time dependent model, i.e., it does not have time information regarding the wind speed profile fluctuations being difficult the wind speed chronological observation [37]. Further, the  $TI$  presents some issues, particularly when the value of  $\bar{u}_{\infty}$  approaches or is equal to zero, the values of  $TI$  are greater than 100%, giving erroneous correction values. Another disadvantage is that urban environments have gusts that significantly affect the standard deviation and  $TI$  value.

Mainly, the turbulence index's drawback is that it considers the wind measurements distributed normally. Moreover, when the model combines the Gaussian distribution with the  $TI$  factor, the wind profile takes negative values, causing a mistake when the wind power generation is calculated. In this way, Woolmington et al. [64] developed a model to characterize the turbulence behavior in the wind profile, called Turbulent Fourier Dimension ( $T_{DF}$ ), and it was compared with the conventional turbulence intensity model, using wind resource measurements in two places in Dublin (Ireland).

Rakib et al. [60] compared the standard IEC 61400-2 parameters with real operation measurements of 5 kW HAWT with two blades and a rotor diameter of 5 m. The study employed three 3D ultrasonic anemometers installed at the height of 15 m on the wind turbine tower. The system was located at the University of Newcastle (Australia). For acquired data values, the study employed WindView software. Wind speed was monitored over twelve months with a frequency of 20 Hz. With real data, Rakib et al. [60] calculated the gust factor  $GF$  and compared it with the standard model. Authors concluded that standard IEC-61400.2 did not represent the gust profile within an urban area. Rakib et al. [65] presents the characterization of the wind resource in urban areas, precisely the vertical wind speed, and compares it with the formulation given by standard IEC-61400 for open land. A horizontal axis wind turbine of 5 kW rated capacity with two blades of 2.5 m long was used in the research. The wind turbine's rated operating parameters were a wind speed of 10 m/s, an angular velocity of 320 rpm at a TSR of 8, and it was mounted at the height of 18 m.

Similarly, KC et al. [63] compared the standard IEC with simulated behavior of HAWT operated in turbulent urban terrain and focused on the effects on the power output and fatigue loads. The wind profile was based on measurements in two different places, Port Kennedy (Australia) and an open area in Östergarnsholm (Sweden). Then, data was processed with software TurbSim v2.00 which can be used as input for FAST software. The 5 kW wind turbine was modeled as aeroelastic in FAST v7.02.00. The wind turbine had two blades, rated wind speed of 10.5 m/s, cut-in wind speed of 3.5 m/s, rated angular velocity of 320 rpm with a TSR of 8. Additionally, the computational model had a passive yaw control system by a delta-wing tail, and the design of the blades counted with the SD7062 airfoil profile over the span.

The blades of the described wind turbine had a length of 2.5 m and were simulated as made of glass fiber reinforced polymer (GFRP). The study concluded that the turbulent model of standard IEC 61400-2

does not represent the actual operation of small wind turbines in turbulent environments. The wind turbine's predicted performance in Port Kennedy using the software FAST, showed that power output increased by turbulent present into wind profile. Still, the blade's root presented more bending moment than the simulation in Östergarnsholm, due to the magnitude and direction fluctuation of wind speed.

Recently, researchers have shown that power generation by wind turbines installed in urban areas presented a reduction between 15% to 30% of nominal capacity. Wind turbine's capacity factor has a value of 10% in open terrain operation; the same wind turbine operating in a turbulent environment has a capacity factor of less than 7% [66]. For these reasons, some researchers compared the IEC standard method with real measurement during operation time to analyze the variation between theoretic conditions and actual conditions.

Dilimulati et al. [66] present recommendations regarding the installation of wind turbines in urban areas. The authors suggest that for deployment of SWTs in urban sectors average wind speed must be at least 5.5 m/s. Additionally, the height installation must be at least 50% higher than the surrounding buildings or obstacles. The hub height must be located 30% higher than the rooftop. Therefore, the installation should be above the turbulent boundary layer.

Pagnini et al. [67] compared the performance of two wind turbines, one HAWT and one VAWT, both had a nominal capacity of 20 kW and were installed in Savona (Italy). The study compared the electric power generation involving the turbulence index with the power generation using the IEC 61400-12-1 standard's statistical method. The study concluded that the manufacturers' curves for both turbines did not represent the real generation. This will depend on the location, the roughness of the installation site, the direction of the wind resource, and the effects of turbulence. The HAWT model presented a more outstanding energy production than the VAWT model; however, the HAWT was more affected by gusts and fluctuations in the wind speed direction.

Lubitz [68] studied the Bergey XL.1 model's behavior, a SWT with a nominal capacity of 1.0 kW and a rotor diameter of 2.5 m. The turbine was mounted and operated in a rural area in Oxford (UK), where the wind resource showed turbulent behavior. The power generation was estimated by measuring the output voltage and the electric resistance of an external load. The author compared the results obtained of  $P$ - $V$  curve with two studies of the same turbine. Additionally, this work presented the results of wind speed frequency and turbulence intensity. The study concluded that as  $TI$  increases at low speeds, power generation also increases; however, when  $TI$  increases at high speeds, power generation decreases.

Ward and Stewart [69] studied the behavior of a wind turbine with a nominal capacity of 2.4 kW, considering the effect of the turbulence index. The authors mainly compared the manufacturer's power-speed curve with the power generation according to the IEC standard and applied the height correction factor for wind speed measurements (Equation (3)). The results showed that electric power generation increased due to the increase in  $TI$  for low speeds. However, when speed increased with the same values of  $TI$ , the turbine's power output decreased, the same conclusion presented by Lubitz [68].

Cooney et al. [70] studied energy production by an 850 kW wind turbine. First, the author described the resource with the wind rose and histogram, then compared the power generation calculated using field measurements with the manufacturer's characteristic curve. Although the turbulence index was not involved in this study's mathematical model, experimental measurements were adapted to the theoretical behavior. Furthermore, that work compared the curves of the real and theoretical power coefficient ( $C_p$ ) and presented the implementation of the Weibull distribution to estimate future energy generation, which was complemented by an economic study of the Levelized Cost of Energy (LCoE) and Net Present Value (NPV).

Carbó Molina et al. [71] studied different turbulence conditions of an H-Darrieus VAWT model in a wind tunnel to identify the turbulence intensity and Reynolds number. For the experiment, the wind tunnel had passive grids to increase the turbulent behavior inside it. Additionally, measurements were

taken in two different wind tunnels with different sizes. The wind turbine scale model had two blades with a 5 cm chord NACA0018 airfoil, a diameter of 0.5 m, an area of 0.4 m<sup>2</sup>, and an angular speed of 1200 rpm to simulate an operational Reynolds. The authors concluded that turbulence intensity had a positive effect on the wind turbine's power coefficient, increasing 20% due to the turbulent index of 0.5% to 15%, which is higher from lower Reynolds and TSR.

Battisti et al. [29] recognized the importance of wind resource characteristics and the wind turbine at different time scales. It refers to the time between two states of wind velocity (direction or magnitude), that for the case of wind turbines, is the time that it spends to adapt for wind velocity changes. The interaction of these time scales provides the integration between the natural phenomenon and a wind turbine's operation. Therefore, the turbine's response to wind condition variations depends on the time scale of the speed fluctuation and the turbine's response characteristics. The authors concluded that the inertial response governs the response time of the turbine. The authors also discussed the requirements for a turbine to operate under variable wind conditions and introduced the Required Rotor Acceleration (*RRA*) and Available Rotor Acceleration (*ARA*). The *RRA* is the acceleration required by the rotor to follow a change of wind speed (Gust). For a fixed geometry and continuous monitoring of the maximum generation point, the *RRA* is expressed as,

$$RRA = \frac{\lambda_{opt}}{R} \dot{u}_{\infty}, \quad (23)$$

where  $\lambda_{opt}$  is the optimum TSR,  $R$  is the radius of rotor and  $\dot{u}_{\infty}$  is the wind speed acceleration. In the case of a large rotor radius, the *RRA* is smaller for any wind acceleration. On the other hand, if the turbine rotation speed increases, a higher acceleration of the rotor is required to track wind acceleration. In this sense, Emejeamara and Tomlin [72] studied the effect of gusts on wind speed profile and the importance of resource tracking technologies for urban applications. The authors used a small-scale VAWT and the *TI* to study the effects of turbulence, which was related to excess energy or fraction of kinetic energy when the wind profile had gusts. The numerical value of excess energy was presented with the indicator of Excess Energy Content (*EEC*) given as [72,73],

$$EEC(\%) = (GEC - 1) \times 100\%, \quad (24)$$

where  $\bar{u}_{\infty}$  is the mean wind speed over 10 min and *GEC* refers to the gust energy coefficient,

$$GEC = \frac{\int_0^T u_{\infty}^3 dt}{\bar{u}_{\infty}^3 T}, \quad (25)$$

and  $T$  takes the value of 10 min. The value of *EEC* can be applied in the energy study to improve the estimation of energy production. The results showed that when *TI* increased, there was additional energy due to gusts in the wind profile. On the other side, the *ARA* is defined as the maximum available angular acceleration when the rotor is free to accelerate under gust conditions with no contribution of the torque applied in the opposite direction (i.e., electric generator's torque); it is expressed as [29],

$$ARA = \dot{\omega} = \frac{Q_{aero}}{I}, \quad (26)$$

being  $Q_{aero}$  the wind turbine torque. Battisti et al. [29] concluded that the *ARA* for HAWTs is one order of magnitude higher than for VAWTs of equivalent radius. This is more notable at low wind speeds, which are more common in urban environments. Finally, two possible scenarios arise from comparing *RRA* and *ARA*. The first one refers to when the turbine can follow the variations in speed and the parameters

established by the control that happens when  $RRA < ARA$  occurs. On the contrary, when  $RRA > ARA$  is met, a rotor acceleration delay is present, and the optimum TSR may not follow the wind variations since the required acceleration is not allowed.

#### 4. Aerodynamic Wind Turbine Rotor

Distributed generation refers to the use of small generation technologies to produce electricity close to the end-users, becoming a more appealing alternative concerning the use of large-scale farms or conventional plants when it comes to the supply of energy in urban and rural areas. Wind power for distributed scale and off-grid applications has been implemented by using turbines of up to 100 kW, commonly denominated as SWTs and, to a similar extent, with turbines in the “medium” size range of 101 kW to 1 MW [74]. Recent trends in the wind energy industry show that distributed generation, below 10 kW, is gaining popularity in rural or isolated areas and urban environments.

The implementation of energy generation policies that allow domestic consumers to sell excess energy into the grid increases the attractiveness of small generation units. Remote areas are another important example of an opportunity to use small wind turbines. The penetration of an interconnected system for the transmission of energy in this type of location must overcome several hurdles, such as geography or economic feasibility. Projections point that SWTs are cost-effective alternatives to conventional non-renewable and centralized generation, for use in applications such as the electrification of rural areas and integrated in hybrid systems with solar PV generation [75]. The success of distributed wind generation, it is bounded by aspects such as electricity generation and transmission costs, restrictions in the required area and the difference in the LCoE when compared with other energy sources [30].

The performance of a wind turbine as a whole depends on several variables that include the operating conditions such as wind and angular speed. The rotor blades’ operation depends on one design element in particular: the airfoil section, which not only fixes the aerodynamic coefficients but also the bending moment of inertia. The recent interest in using wind energy for small-scale applications, e.g., off-grid generation as part of a hybrid system, has driven wind turbines’ design towards rotor diameters of less than 10 m and nominal power below 10 kW. At this size ranges, a conventional airfoil’s behavior is significantly affected by low Reynolds numbers that characterize the flow around the rotor’s blades. This section depicts efforts concerning aerodynamic improvements in SWTs regarding its performance in urban and rural uses.

##### 4.1. Low Reynolds Airfoils

Smaller Reynolds numbers characterizes the flow conditions on small wind turbine blades; therefore, the down-scaling of a wind turbine rotor for the applications in small scale generation presumably requires a careful review of the key aspects of airfoil behavior at low Reynolds and the work that has been made so far, to close the gap of knowledge and help to make design decisions for the conception of efficient small HAWT. The National Renewable Energy Laboratory (NREL) work on wind turbine dedicated airfoils since the early 1990s, consists of the design and study of specially purposed airfoils use of numerical tools [76].

Somers [77] present a design methodology of airfoils for rotors with 20 to 40 m in diameter being one of several publications that report the use of a computational tool based on the potential flow and boundary layer theories. Those tools are used to obtain airfoil geometries from a set of specified constraints, e.g., a specified pressure distribution. For example, the S822 (blade tip) and the S823 (blade root) airfoil sections, designed for stall-regulated rotors with 3 to 10 m in diameter, are obtained with this design methodology [78]. The stated design drivers for this work are a moderate maximum lift coefficient at the blade’s tip and maximized at the root, low profile drag, and a maximum lift coefficient insensitive to

roughness. The results on this set of airfoils report a soft stall behavior, beneficial for stall-regulation and reduction of oscillatory loads under the gusty wind.

The variables of interest for the selection of an airfoil describe the geometry of the section in the form of the relative thickness ( $t/c$ ), and the aerodynamic efficiency, given by the maximum lift-to-drag ratio  $(L/D)_{opt}$ , the corresponding lift coefficient  $C_{l,opt}$ , and the maximum lift coefficient  $C_{l,max}$ . These properties are recurrent in published works; the relevant data has been arranged in Table 5, also showing the flow regime at which the properties are reported and the specified use for each one.

An additional work done by Somers [79] presents an improved series of airfoils: the S833 (for use at the mid-span region of the blade), the S834 (intended for the tip region), and the S835 (designed for the root region), all of them designed for rotors with variable-speed/variable-pitch regulation. Besides being intended for quiet operation, these airfoil geometries aim to provide high maximum lift, independence of roughness, low profile drag, and soft stall behavior.

Giguère and Selig [80] present a series of four airfoils for the intended use at Reynolds numbers between 100,000 and 500,000: SG6040 (root region), SG6041 (primary airfoil), SG6042 (primary airfoil), SG6043 (primary airfoil). These airfoils are designed for maintaining optimum lift-to-drag ratios at varying operating conditions and are characterized on the one hand by high pitching moments, resulting from the flat pressure gradient distribution, usually aimed to mitigate flow separation. On the other hand, the presented analysis shows a non-smooth stall behavior, a characteristic that limits the applicability of the presented airfoils to variable-pitch/variable-speed regulated turbines.

#### 4.2. Airfoil Aerodynamic Aspects

The historical perspective presented by Tangler [81], highlights the importance of leading-edge roughness independence in the design of wind turbines. It points out how the surface degradation in the leading edge region negatively affects several NACA airfoil families' performances used in early wind turbine designs from the 1980s. This work also discusses the phenomenon of laminar separation bubbles concerning wind turbine performance and points how, in the worst case, it can reduce lift while increasing drag.

Laminar separation bubbles can occur due to high suction peaks in a low Reynolds flow over an airfoil; this explains why the requirement of a shallow pressure gradient on the upper surface of an airfoil is a common design constraint for low Reynolds airfoils. Lissaman [82] has discussed this particular mechanism of separation at the beginning of the 1980s; several years before this topic was actively taken into account in the design of wind turbine airfoils.

The reduction of high suction peaks in airfoils can be achieved with a flatter pressure coefficient distribution over the section's upper (or suction) surface. Geometries such as those of the SG60XX set of airfoils are designed under this premise resulting in relative thicknesses of 10 to 16%. At this point, the structural aspect takes relevance as both the works presented in [80,81] related to small wind turbine airfoils to small relative thicknesses. This response to the less strict structural demands that a blade encounters in a small wind turbine opens a new area of discussion, as slender blades can be vulnerable to large deflections deriving in potential issues such as flutter or blade-tower collisions.

The work presented by Selig and McGranahan [83] consists of a careful experimental analysis of six different airfoils that includes the previously mentioned S822 and S834, as well as the E387. Besides giving insight into the nature of laminar separation bubbles with flow visualization, this work uses zig-zag tapes to recreate leading-edge roughness in the experimental campaign. The findings show that leading-edge roughness, as a triggering turbulent flow transition mechanism, can be beneficial in small Reynolds (100,000) most likely by avoiding forming the laminar separation bubble. At higher Reynolds flows



(up to 500,000), the increase in friction drag can outweigh any possible benefit derived from reducing pressure drag.

#### 4.3. Numerical Approaches for Aerodynamic Assessment

It is worth mentioning that extensive and rigorous experimental studies such as the one presented in [83] are not common. Except for a series of publications containing experimental airfoil characteristics [84–86], most of the works on airfoils for small wind turbines are focused on a single airfoil family, a reduced group of airfoils or rely on numerical tools for predicting airfoil characteristics. Henriques et al. [87] present a work in which an airfoil is designed by prescribing not only the load distribution but also the thickness distribution along the chord length of the section. In this case, the airfoil geometry is determined in an iterative way using a panel method software. The resulting airfoil is analyzed using computational studies at Reynolds numbers between 300,000 and 1,000,000 and with an experimental test at a Reynolds number of 60,000.

Most numerical tools for airfoil design via iterative or optimization techniques use software-based on potential flow theory. For instance, Kim et al. [88] implement an airfoil design aiming for low noise emissions and optimal aerodynamics using XFOIL [89], a well-known software based on panel methods. Natarajan et al. [90] use XFOIL for studying the aerodynamic characteristics of an airfoil at Reynolds below 250,000. However, this kind of tool must be used carefully regarding low Reynolds applications. Based on the potential flow theory, the original formulation of a panel method does not account for viscous effects. Then, the approach to airfoil analysis with panel methods places three sources of uncertainty for wind turbine analysis at low Reynolds: (1) under-prediction of drag, (2) over-prediction of the maximum lift, and (3) inaccurate representation of the post-stall behavior.

The disadvantages of panel method models for predicting airfoil characteristics at low Reynolds have been addressed by discussing current aspects of wind tunnel testing for wind turbines and its components, as shown by Van Treuren [91]. A different approach is taken by Grasso [92,93], who presents an optimization work with gradient-based methods and a hybrid approach that uses a genetic algorithm along with a gradient method. The latter author's work favors numerical analysis as a more feasible option for optimization tasks, which are characterized by the inclusion of aerodynamic and structural constraints in what is called Multidisciplinary Design Optimization (MDO).

In this sense, an increasing level of sophistication in the modeling component of current optimization works can be observed. A modified version of XFOIL with an improved description of maximum lift and post-stall behavior is used in [92,93]. Benim et al. [94] use a full RANS solver along with a two-equation turbulence model as part of an airfoil optimization problem, aiming to maximize the torque generation while ensuring a smooth operation. The work presented by Ram et al. [95] consists of implementing a genetic algorithm for the optimization of a small wind turbine airfoil. The optimization aims to maximize lift while minimizing drag, including a bump in the leading edge region to force turbulent transition and recreate the effects of leading-edge roughness. The resulting airfoil is reported to obtain a higher lift to drag ratios than the SG6043 section.

Wata et al. [96] presents an optimized airfoil based on the SG6043 section. New geometry is generated by geometrically combining the baseline airfoil with other airfoils for use in small wind turbines to be analyzed later with XFOIL, considering low Reynolds numbers. Singh et al. [97] propose the design of an airfoil considering the effects mentioned above of low Reynolds and suggest an airfoil shape with a flat upper surface that minimizes the chances of flow separation. Avoiding laminar separation bubbles seems to be a known aim in many recent works on airfoil design for small wind turbines and medium-scale turbines, as happens to be the case of Hall [98].



**Table 5.** Properties of reviewed airfoil sections for applications in small wind turbines.

Designation	$t/c$	$(L/D)_{opt}$	$C_{l,opt}$	$C_{l,max}$	$Re$	Characteristics	Source
S822	16%	50.2–87.0	1.00–0.78	1.06–1.45	100,000–500,000	Tip-dedicated, smooth stall.	[76]
S823	21.2%	75.6	1.03	1.23	500,000	Root-dedicated, smooth stall.	[76,78]
S833	18%	-	-	1.10	400,000	Quiet, primary airfoil, smooth stall.	[79]
S834	15%	78.8	0.75	1.12	500,000	Quiet, tip-dedicated, smooth stall.	[79,83]
S835	21%	-	-	1.20	250,000	Quiet, root-dedicated, smooth stall.	[79]
SG6040	16%	46.0–86.6	1.16–1.13	1.29–1.49	100,000–500,000	Insensitive to L.E. roughness.	[80]
SG6041	10%	51.5–84.4	0.86–0.61	1.15–1.36	100,000–500,000	Insensitive to L.E. roughness.	[80]
SG6042	10%	55.6–105.9	1.10–0.84	1.35–1.52	100,000–500,000	Insensitive to L.E. roughness.	[80]
SG6043	10%	59.4–125.1	1.37–1.10	1.52–1.70	100,000–500,000	Insensitive to L.E. roughness.	[80]
E387	9.1%	57–117	1.16–1.22	1.20–1.27	100,000–500,000	Roughness Stall-insensitive.	[83,86]
T.Urban 10/193	17%	18	1.44	1.76	60,000	High lift, soft stall.	[87]
NACA 63-421	17.3%	93	0.8	1.22	1,020,000	Improved L/D, Reduced noise.	[88]
AF300	14%	14.7–30.0	0.41–1.38	1.06–1.85	38,000–250,000	Delayed flow separation	[97]
USPT2	10%	72	1.2	1.72	200,000	Soft stall & soiling insensitive.	[95]
WTS 1	17.95%	112.79	1.28	1.42	750,000	Designed as a root airfoil.	[98]
WTS 2	17.95%	119.95	1.28	1.38	1,000,000	Designed as a primary airfoil.	[98]
WTS 3	18.13%	115.69	1.25	1.26	1,000,000	Designed as a tip airfoil.	[98]
Mid321a	8%	35–82	-	-	50,000–250,000	Acceptable performance at small $Re$ .	[90]
Mid321b	9.5%	35–83	-	-	50,000–250,000	Acceptable performance at small $Re$ .	[90]
Mid321c	10%	30–84	-	-	50,000–250,000	Acceptable performance at small $Re$ .	[90]
Mid321d	15%	76	-	-	250,000	Best performance at high $Re$ .	[90]
Mid321e	15%	80	-	-	250,000	Best performance at high $Re$ .	[90]

The analysis of turbulent effects is a complex procedure which is often addressed with special care, this is the case of Chillon et al. [99] and their numerical analysis on vortex generators (VG) for wind turbine blades. The authors use source term modeling for the analysis of VG in a RANS environment, and use a 2-equation turbulence model ( $k-\omega$  SST) for flow prediction at angles of attack below  $12^\circ$ . Due to the physics of detached flows around airfoils and the vanes of VG, the authors use a detached eddy simulation (DES) analysis for angles between  $12$  and  $20^\circ$  which corresponds precisely to the stall range.

## 5. Manufacturing Procedures

About 20% of a wind turbine cost comes from the manufacturing of its blades [100]. Therefore, the most common material used in manufacturing SWTs is timber, mainly due to its low cost and suitable properties. These turbines are fabricated mostly by carving or machining blades from solid blocks since timber-laminate composites are costly. Several efforts have been reported to provide easily manufacturable SWTs to allow rural communities for sustainable electrification. This *manufacturability* requires the use of simple manufacturing tools and low-cost procedures to be performed without the use of highly skilled personnel.

Melendez-Vega et al. [101] reported the design of a SWT based on the carving of a standard tube made of polyvinyl chloride (PVC). The authors aimed to generate a low-cost light-weight design for residential use in rural locations. Latoufis et al. [102] proposed a SWT blade made of wood with an estimated cost of 650 EUR for a 2.4 m diameter rotor. Pourrajabian et al. [103] investigated four timber species (i.e., alder, ash, beech, and hornbeam) for use in small blades. The authors included the design and optimization of solid and hollow blades by using genetic algorithms. Other alternatives include the use of metal in windmill's blades, which are often fabricated by rolling galvanized steel [104]. Latoufis et al. [105] investigated the effect of leading-edge erosion on locally manufactured SWTs on power performance and acoustic noise emissions. Eroded wind turbine blades were found to increase 10% acoustic emissions over a range of wind speed from 4 m/s while the power reduction can be up to 23.7%.

### 5.1. Composite Reinforced Materials

However, when the blade length increases (approximately more than 1.5 m), it is challenging to obtain knot-free planks, limiting the use of timber. Here is where composite laminates start to play an essential role by providing an alternative with higher specific properties to reduce inertia [103]. The most common composite materials employed include glass fiber and carbon fiber as reinforcements and polymers (resins) such as vinylester, polyester, and epoxy. Epoxy resins stand out by their most extended shelf life and higher fatigue resistance; however, their main drawback is related to ultraviolet degradation, which implies the need for coatings [106].

In the cases where composite materials are utilized, many of the issues related to the manufacturing of large wind turbines apply to the small-scale case. The standard method for manufacturing wind turbines blades from composite materials consists of machined molds from thin templates, which are then spaced along the span with the gaps filled with the composite system. However, in SWT blades, dimensional accuracy is more critical since an optimum aerodynamic design needs to compensate for the small diameter [106]. Generally speaking, the first composite blades were manufactured by the hand lay-up technology in open molds; however, the technology evolved towards more advanced techniques. In most cases, the fabrication of wind turbine blades is performed as two shells in conjunction with spar or internal webs that are bonded together [107].

As stated by Clausen et al. [104], high-performance wind turbine blades made of composite materials requires variations in chord and pitch along the blade so that pultruded profiles are not suitable. The most common manufacturing techniques for SWTs, once the mold is fabricated, is the Resin Film Infusion

technology (RFI) [107]. RFI includes Vacuum Assisted Resin Transfer Molding (VARTM), also known as Vacuum Injected Molding (VIM), and Resin Transfer Molding (RTM). Vacuum infusion lacks being suitable for in-mass production since it is laborious and requires meticulous work. However, this method has been low-cost and ideal for producing a small number of blades. Besides, it minimizes tooling costs and decreases development time [108]. For high-volume production, RTM appears to be a more suitable technique in conjunction with its variations like Light RTM (LRTM) [106].

Hutchinson et al. [100] demonstrated that by using LRTM in comparison with VARTM, it is possible to reduce the cost by 3% and improve dimensional accuracy by 5.5%. Other improvements were reported as the reduction of resin wastage, infusion time, and void formation; this latter led to an increase in the composite's mechanical performance. Several experimental and numerical works are dealing with void formation, aiming to predict and prevent its appearance [109–113].

The structural design procedure of a low-speed, horizontal axis, bio-inspired wind turbine blade made of carbon/epoxy is presented in [114]. The methodology included the mechanical characterization of the carbon fiber composite material, CFD aerodynamic evaluation of the pressure distribution profile of the blade, and Fluid-Structure Interaction (FSI) simulations to find a configuration which allows balance between aerodynamic and dynamic inertial loads, ensuring an almost undeformed geometry during wind turbine's operation. Then, the authors designed a manufacturing process based on Vacuum Assisted Resin Injection (VARI) for the bio-inspired SWT [115]. The authors performed a study to analyze the resin flow in the manufacturing process simulating different injection strategies. VARI offers advantages over RTM like lower tooling cost, lower injection pressures, and reduced volatile emissions.

Fabrication of blades that mimic some type of biological system is gaining interest in the scientific community. Kaminski et al. [116] developed a bio-inspired gravo-aeroelastic scaling method to structurally scaling wind turbine blades from large wind turbines to 1/100-th scaled models. The scaled model can be low cost, requires light mass while maintaining adequate stiffness. These were fabricated by additive manufacturing inspired by bone growth. Similarly, Ikeda et al. [117] designed and fabricated a SWT with bird-inspired flexed wing morphology, demonstrating that the proposed blades outperformed conventional designs by 8.1% in a proposed Robustness Index. A prototype of the blade was fabricated for validation purposes with a 2-mm-thick hollow structure made of CFRP. Other example of bio-inspiration can be seen in [118–120].

## 5.2. Emerging Manufacturing Techniques

New advances led by the aerospace industry have allowed Automated Tape Lay-up (ATL) and automated Fiber Placement (FP) techniques to be considered for wind turbine blades manufacturing, aiming to reduce costs and ease production. However, as much larger thicknesses are expected in wind turbines blades in conjunction with larger dimensions compared with aircraft composites, some challenges need to be overcome before a broad implementation of such promising alternatives [107]. According to Watson et al. [121], future emerging manufacturing technologies in the wind power sector must focus on reducing costs and manufacturing tolerances. These include fabric-based materials and additive manufacturing for both molds and blades. Additive manufacturing is promising, particularly in the case of small wind turbines, since it is possible to manufacture complex blade shapes without requiring expensive molds [122].

Several types of research have been carried out within this context in recent years. Poole and Phillips [123] used additive manufacturing to fabricate wind turbine blades of Polylactic Acid (PLA). The authors tested several reinforced methods, i.e., pour filled, short fiber infused and pultruded rod-reinforced, concluding that pultruded rod-reinforced was the most suitable. Chaudhary and Prakash [124] fabricated a 0.24-m long blade using additive manufacturing with

Acrylonitrile Butadiene Styrene (ABS). However, the drawback of this technique is related to final product strength and stiffness. Additionally, the use of these additive manufacturing materials raises a concern regarding fatigue resistance issues since they have not been certified yet for wind turbine blades under an existing standard. The solution to this issue may be to use reinforcements for the polymers used as *inks*. Rahimizadeh et al. [125] proposed a systematic scheme based on grinding and sieving to recycle the constituents of the scrap blades and reuse them in a Fused Filament Fabrication (FFF) process for improving the mechanical performance of additive manufacturing components.

Recently, the discussion of the paradox of utilizing petroleum-based materials in the manufacture of wind turbines aiming to be sustainable technologies has led to exploring other alternatives. This includes the investigation of bio-based resins and bamboo [103]. Bamboo-based composites, particularly, have demonstrated suitability by offering higher strength and stiffness over birch constructed laminates [104]. Shah et al. [126] showed that flax is a potential structural replacement to traditional E-glass fiber for small wind turbines. The flax blades were 10% lighter than blade made of glass fiber composites offering advantages in the manufacturing such as no handling itching and inhalation hazardous.

In Table 6, a summary of the reported manufactured small wind turbine is presented indicating material and manufacturing process when reported.

**Table 6.** Noncommercial manufactured small wind turbines.

Blade Length (m)	Blade Weight (kg)	Material	Manufacturing Process	Source
NR	5.5	E-glass/Polyester	NR	[127]
0.24	4.8	ABS	3D printing	[124]
1.9	NR	Carbon fiber/Epoxy	VARI	[115]
9.6	NR	Composite materials	NR	[128]
3.5	NR	Flax/Polyester	LRTM	[126]
3.5	NR	E-glass/Polyester	LRTM	[126]
2.5	7.8	Glass fiber/Epoxy	Hand layup/vacuum bagging	[129]
NR	NR	PVC	NR	[101]
3.2	NR	Carbon and glass fiber	VARTM	[126]

## 6. Control Systems Approaches

This section presents several works related to both active and passive blade and rotor control systems. As it has been throughout this review, the studies shown in this chapter are limited to SWTs and does not include control techniques and technologies concerning the generator. Instead, the focus is on HAWT blades, especially for pitch, yaw, and stall control techniques.

An innovative blade design is presented by Xie et al. [130], this blade's outer section can be folded out of the rotor's plane to regulate the pitch of the blade and, thus, control the energy conversion efficiency. In a posterior work made by the same authors, this wind turbine was built and tested in a wind tunnel; the results showed that the maximum power coefficient could be reduced by up to 82.8% by fold control [131]. Hatami and Moetakef-Imani [132] present an improvement for a small scale HAWT pitch control made by implementing a Self-Tuning Regulator (STR) into it. The resulting pitch control regulates the rotor speed fluctuations above the rated wind speed in a better way since it can adjust the controller gains in real-time. The wind turbine was modeled with FAST; this model estimates the wind turbine parameters, and the obtained information is used to adjust the gain of a PDI controller for the pitch of the blades.

The work presented by Rocha et al. [133] demonstrated that pitch control has a significant effect on the performance of urban installed wind turbines. BEM theory was used to model a HAWT with a fixed TSR. Different blade pitch angles and analysis of variance demonstrated that a blade pitch control system could be an effective method for improving the wind turbine's performance in urban conditions. A comparison

between two different control systems and their influence over flicker emissions, voltage fluctuations, and mechanical loads is presented in Mohammadi et al. [134]. Yaw controlled 10 kW HAWT, and an electromechanical model simulates a stall-controlled 10 kW HAWT by using different software. It was concluded that the stall-controlled wind turbine provided better results in terms of flicker emissions, voltage fluctuations, and mechanical loads than the yaw-controlled one. To better accommodate the nonlinearities of wind turbine systems, Civelek [135] propose a fuzzy logic controller for blade pitch. This controller's coefficients are optimized with an advanced genetic algorithm and resulted in better output power stability. The folding of the blade also reduces the rotor's diameter and thus, the amount of energy available for exploitation is also reduced.

Khaled et al. [136] presented a study related to how the performance of a small scale HAWT is affected by the length and the cant angle of a winglet. Different designs, lengths, and cant angles of winglets were optimized by using an artificial neural network while CFD simulations were made to measure the influence of said winglets in the  $C_p$  and thrust force of the wind turbine. The best results were obtained for a winglet length of 6.32% of the rotor radius and cant angle of  $48.3^\circ$ .

Venkaiah and Sarkar [137] developed a free fuzzy feedforward PID pitch controller for HAWT. BEM theory was used to estimate the aerodynamic load acting on the blade and determine the maximum power capture pitch angle. An electrohydraulic actuator is controlled by the proposed fuzzy feedforward PID controller that achieved a performance index of 0.08606, 0.08849, and 0.09809 with normal leakage, high leakage, and very high leakage, respectively. Siavash et al. [138] reported a study where a small wind turbine was equipped with a controllable nozzle-diffuser duct that surrounds the rotor; the mechanism controls the speed of the flow and the drag forces acting on the turbine structure. The duct consists of a fixed ring and a diffuser which can rotate on each other. This experimental turbine was tested in a low-speed wind tunnel with the duct in different configurations. The results showed that the controllable nozzle-diffuser augments the power output up to 50% and the rotor speed by up to 61%.

Plasma actuators are devices that can locally ionize the air and thus alter the speed and direction of the surrounding airflow. The work reported by Jukes [139], a plasma actuator control system, based on a Surface Dielectric Barrier Discharge (SDBD), was implemented on a small scale HAWT. The study determined that the flow separated from the blade's suction surface radially outwards from the blade root as the TSR is reduced. Placing plasma actuators in different SWTs blade areas allows energizing the boundary layer, reducing flow separation in the middle to tip sections of the blade. It can reduce the torque due to aerodynamic drag by up to 24%, proving the feasibility of implementing smart rotor control based on plasma actuators.

A novel mechanism for improving rotor energy capture and load performance consist in the use of rotor blades with bend-twist coupling. This technology has been explored numerically for inducing a passive torsional response in the blades of the rotor in different applications; for instance, the work of Maheri et al. [140] reports increments in *AEP* of up to 13% while Nicholls-Lee and Turnock [141] shows increments in *AEP* of 2.65% for a rotor with variable pitch and bend-twist coupling.

Similar works with a numerical approach have been performed on different multi-megawatt wind turbines such as Barr and Jaworski [142], which reports a 14% increase in *AEP* for a 5 MW rotor. Passive bend-twist coupling incorporates several technologies for blade torsional actuation, including composite material anisotropy, with and without tow steering and, geometrical approaches based on swept blade designs as demonstrated in the aeroelastic and structural design works of Capuzzi et al. [143–145]. The use of this passive technologies is not limited to direct power increase, as some studies such as that of Zahle et al. [146] have evidenced their effectiveness for load alleviation, using numerical simulation in large rotors and combining active blade pitching for energy capture in the below-rated range with passive bend-twist coupling for load alleviation in the above-rated range. Given the complexity in modeling for this kind of design problems, several authors have opted for

novel optimization techniques, such as Restrepo-Montoya et al. [147], who proposes a metamodel-based methodology to design laminates with bend-twist coupling effect by means of genetic algorithms (GA) and artificial neural networks (ANN) integrated with a finite element model (FEM) capable of defining the stacking sequence that a laminate needs to reach a certain twist angle when submitted to bending load. This kind strategy resembles to that of Herath et al. [148] who uses a GA approach for optimization of composite layup in a morphing blade with induced bend-twist coupling by differential stiffness elements. In other cases, the application of GA is used in the joint design of rotor geometry and structures taking global parameters such as *AEP* or *CoE* as the cost function of the optimization exercise [149–151].

Although the focus of this survey is on HAWTs, there are several works on blade controlling of VAWTs whose principle may potentially be applied to HAWTs. Bianchini et al. [152], a BEM model, was used to explore different pitch control strategies for VAWT rotors. The BEM model was successfully validated via CFD simulations, and it was determined that an optimized pitch could result in better exploitation of higher-lift parts of the blade's polar during the rotation. Three pitch optimization strategies were presented and concluded that wind speed-dependent strategies to optimize the pitch angle produce a greater annual energy output but the increased complexity of those systems might not be compensated. The authors also concluded that a fixed pitch optimization approach could result in a cost-free improvement of the VAWT.

An intelligent pitch angle control for an H-VAWT is presented by Abdalrahman et al. [153]. The  $C_p$  of the turbine is calculated with data obtained by CFD simulations of an H-VAWT blade at different TSRs. The results of these simulations were used to make an aerodynamic model of the rotor. This model was then used to create an intelligent blade pitch controller for each blade's pitch angle by using an artificial neural network. The obtained controller resulted in superior power output for the VAWT when compared with a standard PDI controller.

Sagharichi et al. [154] made a work that consisted of four different pitch functions with different amplitudes used to evaluate the relationship between the pitch angle and the self-starting performance for both a fixed pitch and a variable pitch H-VAWTs. All cases had better results with the amplitude of case 1 is reported to have achieved the least time required for starting and to have an increase of 34% in power.

## 7. Hybridization and Integration

One of the main disadvantages of wind energy is its variability in time due to the intermittent nature of the wind speed, therefore, the energy distribution also has the same behavior. For this reason, wind speed is classified as a variable renewable energy source (VRE) [155]. There are two ways to solve the effects of resource variability and guarantee energy security: (1) storage systems [156] and (2) electrical interconnection systems [157]. However, insufficient storage and the absence of interconnection in some areas increases the uncertainty that the installed capacity adequately supply the energy demand [158].

By composing a hybrid system that integrates wind generation and other renewable sources, including a storage system such as a battery bank [15], it is possible to meet the energy demand of a region [159]. Koutroulis et al. [160] found that systems composed of solar photovoltaic (PV) panels, wind turbines and battery banks (BB) meet the demand of unconnected sectors to transmission networks, even achieving lower values in capital and maintenance costs than systems that have only PV or WT.

Additionally, it is possible to facilitate the integration and complementary of VREs through the interconnection of spatially distributed generators or the use of complementary generators, operations that apply monitoring or response to demand, oversizing of storage systems with hydrogen, the use of electric vehicles as storage concept [161], generation prediction [33], or adaptive droop control [162].

The concept of complementarity between renewable resources is of evident relevance in this context, mainly as an indicator of the energy security for a particular region. Renewable resources such as sunlight and wind depend on the space and time of the area where the energy system is operated. Factors such



as height above sea level, temperature, humidity, topography, or presence of clouds, directly affect the generation of VRE.

This condition does not depend on whether the resource is renewable or not, the accessibility of fossil fuels in the region or its surroundings is also evaluated. However, it is a reality that the wind resource is present in all regions to a lesser or greater extent, making it essential for complementarity in electricity generation [158].

Spatial complementarity occurs when two or more energy sources coincide in a specific region, and temporal complementarity refers to periods of availability when complementary there is in the time domain. In this way, the concept of space-time complementarity is generated, where multiple energy sources are simultaneous both in time and space [33].

Jurasz et al. [33] presented some correlations and indices to quantify the amount of energy complementarity. Among these correlations are Pearson's, Kendall's, Spearman's rank correlation coefficients, canonical correlation analysis (CCA), and cross-correlation. In the case of the indices, the complementary index of wind and solar radiation (CIWS) and an index that integrates the geographic regression model and the principal component analysis (PCA) stand out.

Mahesh and Sandhu [163] shown a summary of the complementarity of solar and wind resources, the authors dealt the mathematical modeling, system constraints when integrating battery banks, and the reliability of hybrid renewable energy systems. Shivarama Krishna and Sathish Kumar [164] affirmed that the hybrid systems are the best option for building modern power grids, including economic, environmental, and social benefits.

Chauhan and Saini [165] presented a summary of the possible configurations in the integration of renewable energies, options of storage technologies, the mathematical modeling of wind systems, micro-hydroelectric systems, PV solar systems and bioenergy systems, in addition to a summary of the numerical methods to optimize the sizing of hybrid renewable energy systems and control systems for energy management. Siddaiah and Saini [166] also presented some optimization techniques and identified the renewable sources of each study, the objective function of each algorithm, and whether the search approach was economic, environmental, social, or technical.

Tezer et al. [167] evaluated optimization methods for hybrid systems, some objective functions, and emphasized in some hybrid optimization models. Kajela and Manshahia [168] summarized the types of renewable energies, their advantages and disadvantages, the importance of hybrid systems, some typical hybrid renewable energy systems (HRES), the modeling of objective functions, their restrictions, and the computational tools for optimization in sizing.

One of the challenges in the integration of wind and solar systems is related to the compatibility in voltage, where the photo-voltaic solar system responds faster than the wind system [169]. In this way, studies have been carried out addressing this integration from the control of electrical variables. Chaib et al. [169] presented a control system that coupled the wind and solar systems through two switches that converge on a DC bus. In the same aim, Huu [162] developed an adaptive control for a storage system for DC distribution networks. The authors introduced DC distribution micro-grids, the conventional droop control method, the battery storage system model, and the adaptive droop method.

Sinha and Chandel [170] summarized the trends in the optimization methods for hybrid systems, focused on solar and wind technologies, the authors also presented a comparative table showing the strengths and weaknesses when using iterative approaches, graphic models, probabilistic approximations, linear programming, and trade-off methods. Khare et al. [171] also summarized the systems composed of solar and wind technologies, and focused on the review of evolutionary techniques for optimization, where genetic algorithms (GA) and particle swarm optimization (PSO) stand out [7]. Al-falahi et al. [172] presented the developments in optimization methodologies for sizing HRES, mainly focused on the



integration of wind and solar systems, and described the comparison between the different objective functions and restrictions of each method.

Several authors highlight the low cost of PV systems into HRES systems when the hybridization sizing includes also wind energy generation. Maleki and Pourfayaz [173] carried out the sizing of an autonomous hybrid solar-photovoltaic/wind/bank-battery system using MATLAB and various evolutionary algorithms such as PSO, tabu search (TS), simulated annealing (SA), improved particle swarm optimization (IPSO), improved harmonic search (IHS), a hybrid model between IHS and SA, and artificial bee swarm optimization (ABSO). The best results obtained by the authors shown that PV/BB systems reached fewer total annual cost (TAC) values than the WT/BB systems.

On other hand, Torres-Madroño et al. [7] presented the sizing of PV/WT/BB hybrid system, using a computational tool on Python that implemented GA and PSO methods with single and multi-objective function, involving TAC and levelized cost of energy (LCoE). The authors concluded that when the optimization method searched the best configuration with economical criterion (TAC or LCoE), the HRES systems had 100% of photo-voltaic generation, obtaining LCoE values between 0.160 and 0.287 USD/kW-h, depending on the energy demand case.

In the same way, Mayer et al. [174] studied a novel method for sizing a hybrid system based on the environmental impact throughout the life cycle of the equipment involved in the HRES. The authors employed the multi-objective function with the mentioned environmental factor and the net present cost (NPC) by the GA method. The HRES configuration took into account photo-voltaic solar energy, wind energy, solar heat collector, heat pump, heat storage, battery bank, and heat insulation thickness. The study concluded that if the configuration got away from economic optimum to reduce the environmental impact, the installed photo-voltaic capacity increased, being the most profitable way to reduce emissions.

## 8. Assessment of Currently Available SWTs

Some of the most relevant concepts for aerodynamics, wind resource, manufacturing and control strategies that have been discussed in previous sections are now analyzed from energy generation and energy cost point of view. This analysis is based on three indicators: the *AEP*, the capacity factor, (CF), and the CoE. The definition in Equation (7) is adopted for the calculation for the *AEP*. The wind resources under analysis have been defined as hypothetical cases by assuming Weibull probability distribution functions following Equation (4). The difference in mean wind speed and shape factor for each distribution is expected to describe wind conditions at sites of different characteristics; however, these do not correspond to actual measured data and should be considered when interpreting the subsequent results. Likewise, the power curves for the considered wind turbine models are taken as provided by certification reports although the real data is naturally subject to variations that might affect the outcome of the calculations. The ratio between the annual energy output and the annual energy output at rated conditions is given by the CF, defined in [175–177] as:

$$CF = \frac{AEP \text{ (kWh)}}{P_{rated} \text{ (kW)} \cdot 8760 \text{ h}} \quad (27)$$

The model for the CoE is based on the annual fixed cost ( $C_{fix}$ ) and the operation and maintenance cost ( $C_{M\&O}$ ), both of them estimated on a yearly basis. The final definition is given by:

$$CoE = \frac{C_{fix} + C_{O\&M}}{AEP} \quad (28)$$

The calculation of the fixed cost is based on a simple payback time analysis, assuming a 6% interest rate p.a. and a 10 year payback period; this results in a 13.6% annuity for the yearly payment of the initial investment. The initial investment represents the installed costs, assumed as 7500 USD/kW; similarly, the value of  $C_{M\&O}$  is assumed as 40 USD/kW. All of the data on wind turbine cost is directly adopted from official sources [74,178,179] and it must be mentioned that the availability of information on actual project costs as seen by manufacturers and operators is scarce and varies from year to year. In this sense, the results from preceding calculations are based on averaged values for the sake of illustration on typical wind turbine costs.

### 8.1. Results

Six different wind turbine models are considered, and their characteristics are shown in Table 7, including the manufacturer, model, rotor diameter  $D$ , swept area  $A$ , rated power  $P_{rated}$ , rated wind speed  $u_{rated}$ , cut-in speed  $u_{in}$ , cut-out speed  $u_{out}$ , and control type (yaw, pitch or brake control). *Model 1*, for example, corresponds to a machine with a wooden built rotor that points to a low-cost manufacturing. *Model 6*, corresponds to a modern SWT with a simplified blade geometry while *Model 3* corresponds to SWT with a rotor specially designed to endure strong winds.

**Table 7.** Wind turbines models.

Model	Manufacturer	Model Name	$D$ [m]	$A$ [m <sup>2</sup> ]	$P_{rated}$ [kW]	$u_{rated}$ [m/s]	$u_{in}$ [m/s]	$u_{out}$ [m/s]	Yaw Control	Pitch Control	Brake Control
1	Latoufis et al. [102]	2.4 m-HP	2.4	4.5	0.53	10.5	3	N/A	Passive	Fixed-pitch	N/A
2	Xzeres [180,181]	Skystream 3.7	3.7	10.9	2.1	11	3.5	16.5	Passive	Fixed-pitch	Regulated rotor brake
3	Kingspan [182]	KW6	5.5	23.7	5.2	11	3.5	N/A	Passive	Fixed-pitch	Over-speed protection
4	Endurance [183]	S343	6.4	31.9	5.4	11	4.1	17	Passive	Fixed-pitch stall regulated	Rotor brake
5	Enair [184]	E200	9.8	75.4	18.0	11	1.85	30	Passive	Active	Regulated rotor brake
6	Bergey [25,185]	Excel 10	7.0	38.5	8.9	11	2.5	N/A	Passive	Fixed-pitch	Over-speed protection

It is expected that the diversity in the selected turbines have a direct impact the CoE, as each machine's sophistication should impact the capital costs consequently. One aspect common to all models is these start rated power operation at wind speeds around 11 m/s, a typical rated wind speed for places with adequate wind resources. In contrast, the behavior of power in the above-rated wind speed range, as shown in Figure 3, is different for each model.

Some turbines reach maximum power above 12 m/s (i.e., for *Model 2*, *Model 3*, *Model 4*, and *Model 6*) or present power drops for high wind speeds as is the case for *Model 4*. With a similar intention, five different wind resources are adopted for the CoE calculation. These are based on the Weibull probability distribution and are illustrated in Figure 4.

According to Figure 3, the turbines corresponding to *Model 1*, *Model 2*, *Model 3*, and *Model 4* are characterized by relatively smaller power ratings, ranging from 530 W for *Model 1* to 5.4 kW for *Model 4*,

whereas *Model 5* and *Model 6* are both situated above the 8 kW threshold in terms of rated power. *Model 1* has a significantly smaller cost compared to the remaining models, not only because of its size, but also because it has been specifically designed as a low-cost solution for rural electrification. The influence of the material and manufacturing techniques is still yet to be verified; nevertheless, a significant drop in capital cost is expected when comparing more sophisticated blade manufacturing techniques for high-performance composite materials to manual and simpler manufacturing techniques for cheaper materials such as wood.

A wide distribution in velocity magnitude characterizes the wind resources for *Case 4* [67] and *Case 5* [35]; this kind of resource, typical for coastal and open areas and for flat places, is highly variable, as consequence the *AEP*, shown in Figure 5, is consistently better in these cases for each wind turbine model. The corresponding Weibull distributions (see Figure 4) show favorable frequencies for wind speeds at both the below-rated and above-rated wind speed ranges.

Both *Case 1* [35] and *Case 2* [60] reveal a lower performance, most likely associated to the prevalence of wind speeds below the typical cut-in values for the considered wind turbines. A smaller degree of variation is also observed, compared to the previously discussed cases, which have significant production in the beyond-rated range. For *Case 1* and *Case 2*, a typical wind turbine model can be expected to deliver most of the *AEP* by operating within the below-rated range, which is at wind speeds between cut-in and rated values; this is reflected by the corresponding capacity factors, shown in Figure 6.

The economic analysis presented here considers capital costs for each SWT, including operation and maintenance costs, without incorporating the machine's lifespan. The simple CoE, in USD/kWh has been estimated for each *Model* and *Case* with the model described at the beginning of the section.

An interesting result is the CoE for *Model 1* shown in Figure 7, with lower values than any of the other models and regardless of the wind resource. The low costs associated to wooden blade manufacturing and simplified wind turbine construction can be pointed as the driving factors for this result.

The results for *Model 5*, with a nominal power of about 17 kW, show the second-best performance in terms of CoE, particularly when considering adequate wind resources, such as those of *Case 4* and *Case 5*; in addition, it must be mentioned that this wind turbine makes use of a variable pitch control, resulting in superior rotor conversion efficiency when compared with other models. The wind resource of *Case 3* [35] results in *Model 5* having a competitive CoE, and this may be attributed to more widespread distribution of wind frequencies.

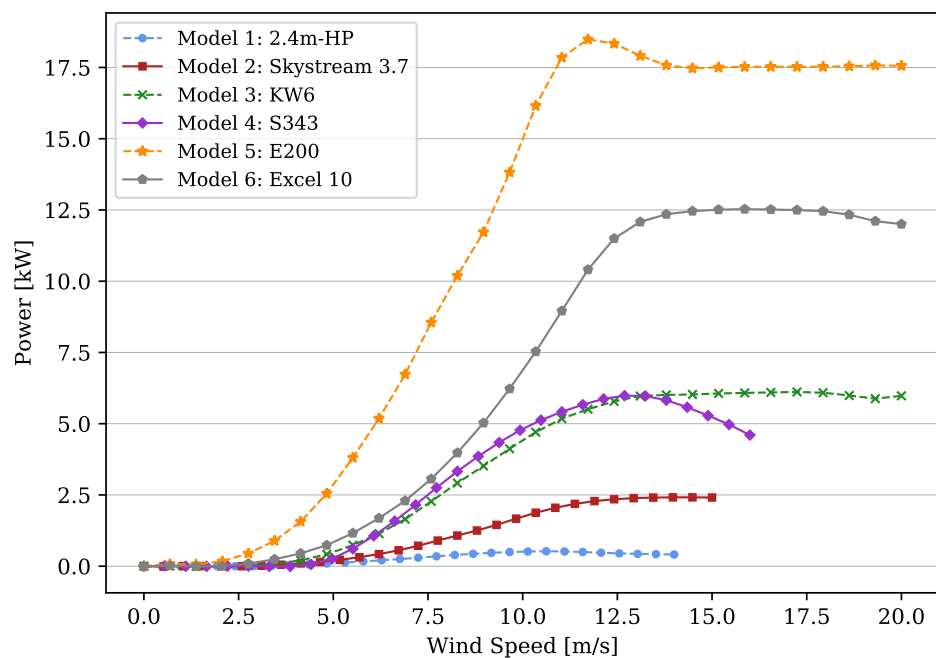


Figure 3. Power curves for reported wind turbine models.

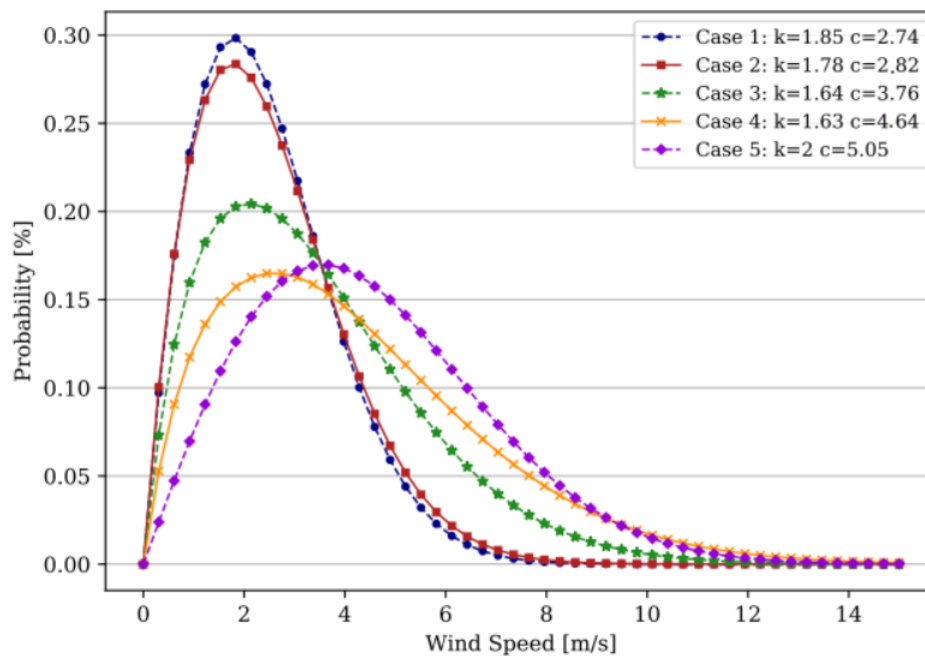


Figure 4. Probability distributions for the wind resource cases [35,60,67].

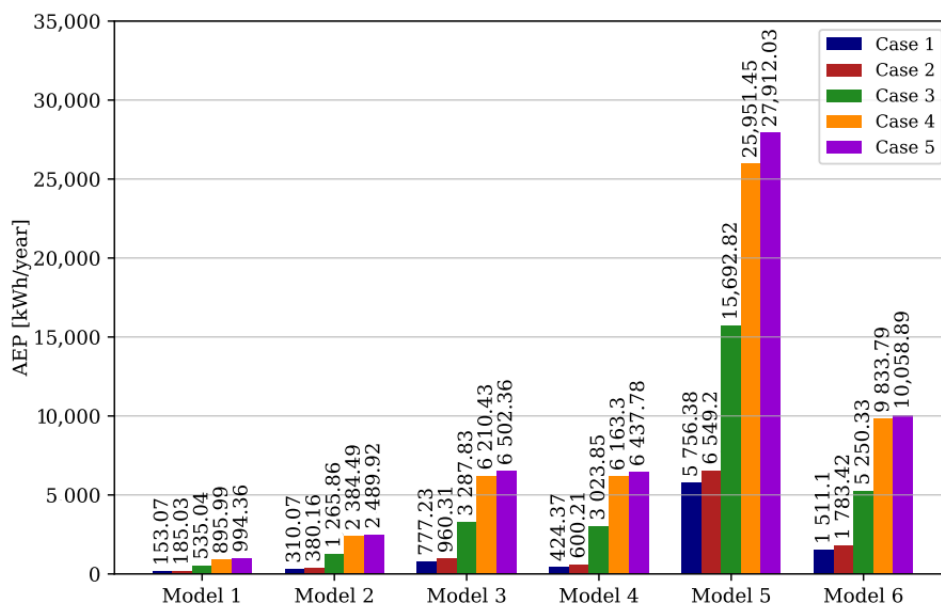


Figure 5. Estimation of AEP in kWh for different wind turbines and wind resources.

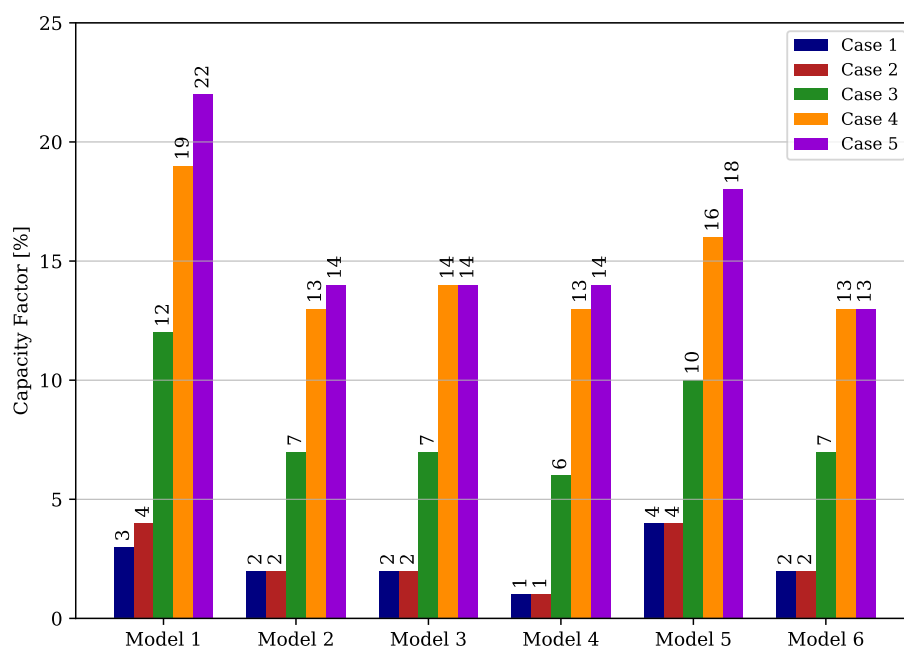


Figure 6. Calculated capacity factors.

The *Model 6* presents a similar performance to that of *Model 5* but with slightly higher CoEs as the AEP reduces by almost a half. Such a reduction in energy output can be attributed to the fact that the rotor of *Model 6* has blades with fixed pitch and apparently constant twist and chord distributions. Such a simplified rotor geometry can be expected to result in a smaller power output but, the associated reduction in wind turbine cost compensates the cost of electricity as shown in this analysis.

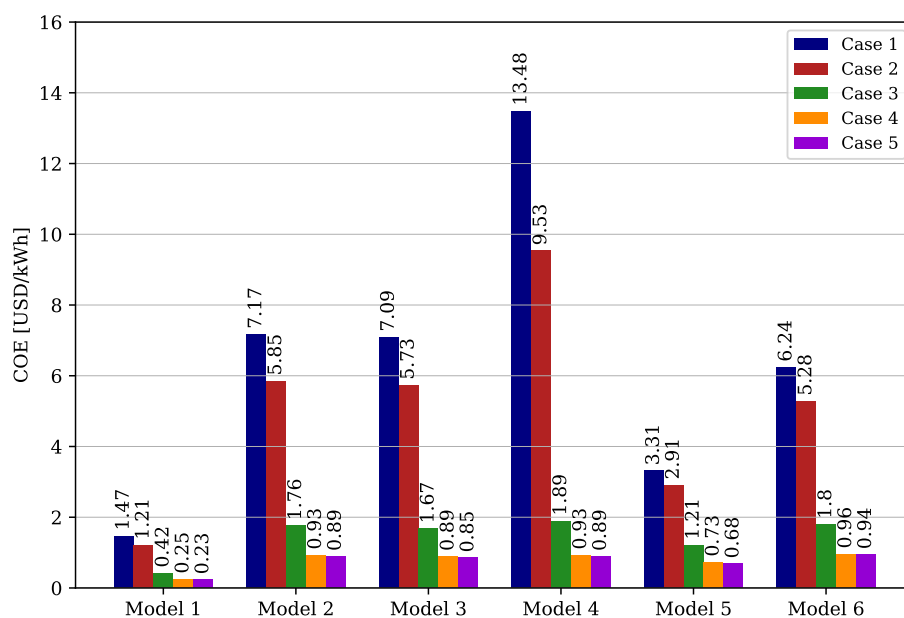


Figure 7. Calculated Cost of Electricity in USD/kWh.

The wind resource of *Case 1* has resulted in an interesting set of CoEs, showing the highest variation with respect to the wind turbine model. A similar outcome is observed for *Case 2* which indicates that the narrow probability distributions shown earlier in Figure 4 results in a CoE that is highly dependent on the shape of the power curve and on the cut-in wind speed for each particular wind turbine model.

The relative similarity in CoE observed for *Case 4*, *Case 5*, and *Case 3* can be attributed, under the same reasoning, to the wider probability distributions for these three wind resources. The data for *Model 4* in Figure 7 shows a difference in the values of CoE, with significantly higher costs for wind resources with narrow probability distributions (*case 1* and *case 2*). It must be said that *Model 4* is characterized by a relatively high cut-in wind speed and a power reduction in the above rated-range, associated to the stall-regulated blades.

In summary, this analysis reveals that if a low-cost turbine can achieve a modest power output for a set of variable conditions, the low-cost factor can significantly help bring down the CoE, with moderate sensitivity to the wind resource variability. For models produced with more sophisticated manufacturing processes and materials, such as *Model 2* to *Model 6*, a poor matching between the power curve and wind resource inevitably results in lower capacity factors. This could drive the CoE to very high values, rendering the machine disadvantageous in sites with small average wind speeds and little variation.

## 9. Conclusions

This review has tested several hypotheses about the current state of the five discussed topics. For wind resource assessment, this review shows that the existing literature focuses on typical wind speed estimation, present wind velocity consideration in standard IEC, and finally, in studies of the operation under turbulent environments. This shows that previous studies have focused on issues that affect rotor performance, airfoil design, and methodologies for flow analysis for rotor aerodynamics.

Regarding manufacture, this paper demonstrated that many works' current aim is to keep the cost as low as possible. However, in some works, the recent tendency is to use advanced materials to improve efficiency. For control systems, this review shows that most published articles have been reported on active control systems for SWTs and that passive control techniques remain mostly unexploited. Finally,

this study presents the complementarity of wind technology with other renewable energy generators, introducing the sizing and control of hybrid micro-grids systems.

The analytical model presented by Equation (1) is a first approximation for a value of mean wind speed. This can be used to estimate the critical load on blades or other mechanical components. However, the log-law model must not assess the power generation for a wind turbine because it does not depend on the time; for this reason, the final estimation of power output will not be the right approach. The design of a wind turbine system requires an energetic study, and the approach given by Equation (7) is ideal for estimating the total energy over one operation year.

Additionally, the most frequent wind speed of Weibull or Rayleigh distribution can be used to calculate the critical operation load with the integration of safety factor under designer's criteria or following the IEC standard that presents  $u_{ref}$  in Table 4. However, when the project and design request is an accurate estimation of power energy and load, the third approach by CFD models is usually employed. Compared with log-law and statistical models, it has a more computational cost and time investment to reach the aim.

Generally, in the studies reported in this work, the standard IEC 61400-2 does not represent the real operation features to small wind turbines that work in urban environments. However, the importance of mathematical models given by standard is useful to designers for conceptual design when SWTs operate in open areas. Moreover, this standard serves as a start point to implement correction models for SWT in urban places.

The majority of researchers compare the IEC standard with their studies involving experimental methods where wind tunnels and wind turbine models or real measurements during operation are used. The criteria for selecting one of these methodologies are related to the required accuracy and the state of maturity of the project.

Some of the studies recognized that the gust effect has additional energy that the wind turbines can extract in urban areas; this is evident by the indicator EEC presented by Emejeamara et al. [73]. However, the excess of energy is limited by wind systems' capacity to track or adapt their performance as function of change of wind speed either by direction or magnitude. For this reason, Battisti et al. [29] presented the reaction capacity of a wind turbine, and its relation with the time scales of response, the time scales of change wind speed, the acceleration required by the wind turbine to adapt to wind speed acceleration, and the maximum acceleration permissible to reach by the turbines.

All of these factors [29] converged in wind tracking index WTI, which is the quotient between ARA and RRA. If WTI is greater than or equal to 1, the turbine will accelerate to following the control parameters. Still, if WTI take values less than 1, the wind turbine will have a critical operation and will not be reactive to magnitude and direction wind fluctuations. In particular, higher ARA are obtained for HAWT at higher speeds; thus, WTI is higher to HAWT than VAWT, in this way these type of turbine is more reactive and enabled for tracking gust. In general, small diameters are required to operate in areas which require a rapid reaction [29].

When implementing conventional airfoils in low Reynolds conditions (predominating in the operation of small wind turbines), some of the main issues are laminar separation bubbles, causing early flow transition or causing separation from the leading edge of the airfoil. This phenomenon decreases lift while increasing drag considerably, which is the less convenient wind turbine blade behavior.

Wind turbines' operation can become less efficient due to erosion in the leading edge of the blade; therefore, an airfoil with design properties that are insensitive to leading-edge roughness is more convenient for wind energy applications with low Reynolds flows. Several works impose the constraint of shallow pressure distribution over the airfoil's upper surface to avoid adverse pressure gradients that result in trailing edge separation. In this case, the design problem is based on inverse methodologies for determining airfoil shape that satisfies a prescribed pressure distribution.



Although not many works are published regarding blade and rotor control focused on SWT, this review shows the great variety of technologies studied in recent years: from simulations of different yaw or pitch controllers to plasma actuators to control flow separation to folding blades and shrouded rotors. Many of the reviewed works for rotor control show simulation techniques and theories. For these simulations to be accurate for SWT applications, the inputs related to wind conditions are critical, considering the available wind resource requirements on the environments where STWs are usually implemented.

This shows the importance of accurate and reliable wind resource assessments and measurements to develop and implement appropriate control techniques on SWTs successfully. A relatively small number of articles were published on blade and rotor control systems made explicitly for SWTs. This highlights an issue with the studies made on SWTs that tend to scale down the same technologies used for large-scale wind turbines and expect them to work similarly. This ignores the differences between large and small scale wind turbines regarding aerodynamic considerations and the wind resource's particularities on the usual environments where SWTs operate.

Regarding the operation, feasibility concerns are raised in wind generation systems based on SWTs, both for grid-connected or off-grid operation. In grid-connected applications, the required electrical connections and access to the installation zone represent an economic barrier. Conversely, when the system operates off-grid, instrumentation for wind speed measurement and civil construction foundations must be considered in the project since these often imply high costs [35]. These costs may be unattractive for rural and urban applications both in grid-connected and off-grid projects if generated power is not enough. Among technical challenges of all diverse nature, such as noise or performance, certification is a crucial aspect in which progress must be made, considering it is essential to opt for government incentives. Furthermore, the cost of accredited testing and certifications are pointed as a critical hurdle given the high price that such processes can reach for a single small wind turbine model.

Despite that PV systems stand out with fewer cost than SWTs, the economic study carried out by CoE in this review show that depending on the wind resource and the wind turbine model, the CoE values can be similar to LCoE value found in previous works. It is the case of the SWT Model 1 on the wind speed profile Case 5, where it reached a CoE value of 0.23 USD/kW-h, which is into the range of LCoE values obtained by Torres-Madroño et al. [7] (0.160 o 0.287 USD/kW-h) for photo-voltaic/battery systems.

However, it is important to mention that the analytic approach given by this review about CoE doesn't have the energy demand in its formulation. Moreover, the literature studies took the temporal wind speed profile in some cases instead of the PDF formulation, like Section 8 here presented. When accurate formulation and results comparing PV and wind generation, the works mentioned in Section 7 are advised.

Reducing the difference between the demand and supply of energy and keeping the cost of electricity at low levels within a minimum impact on the environment are significant concerns regarding the development of generation technologies. In this sense, innovation has brought down costs and increased the availability of renewable power sources, where wind turbines and solar photovoltaic (PV) panels are the leading energy technologies to non-conventional renewable electricity production [186].

In particular, SWTs can be split into two market sectors: (1) machines devoted to supplying electricity in remote areas, and (2) grid-connected applications. The first one concerns the use of SWTs in rural areas, mostly for off-grid consumers, either alone or in conjunction with other types of renewable energies. The reduction in capital and operational costs is paramount, aiming to provide reliable energy. The price cannot be overwhelmed by the value of the connection to the grid. Additionally, such remote consumers often lack economic resources to afford high costs. Regarding the second sector, the motivation is to use renewable sources harvesting on-site wind resources to be self-sufficient and, in surplus scenarios, provide energy to the grid through the so-called smart meter technologies [30].

**Author Contributions:** Conceptualization, C.N.-L. and J.S.-P.; methodology, J.L.T.-M., J.A.-M., D.R.-M. J.M.T.-A., C.N.-L. and J.S.-P.; validation, J.L.T.-M., J.A.-M., D.R.-M. J.M.T.-A., C.N.-L. and J.S.-P.; formal analysis, J.L.T.-M., J.A.-M., D.R.-M. J.M.T.-A., C.N.-L. and J.S.-P.; investigation, J.L.T.-M., J.A.-M., D.R.-M. J.M.T.-A., C.N.-L. and J.S.-P.; writing—original draft preparation, J.L.T.-M., J.A.-M., D.R.-M. J.M.T.-A., C.N.-L. and J.S.-P.; writing—review and editing, J.L.T.-M., J.A.-M., D.R.-M. J.M.T.-A., C.N.-L. and J.S.-P.; project administration C.N.-L. and J.S.-P.; supervision, C.N.-L. and J.S.-P. All authors have read and agreed to the published version of the manuscript.

**Funding:** This research has been developed in the framework of the “ENERGETICA 2030” Research Program, with code 58667 in the “Colombia Científica” initiative, funded by The World Bank through the call “778-2017 Scientific Ecosystems”, managed by the Colombian Ministry of Science, Technology and Innovation (Minciencias), with contract No. FP44842-210-2018.

**Conflicts of Interest:** The authors declare no conflict of interest.

## References

- IEA. *World Energy Outlook 2019*; Technical Report WEO—2019; International Energy Agency: Paris, France, 2019.
- Ahmad, T.; Zhang, D. A critical review of comparative global historical energy consumption and future demand: The story told so far. *Energy Rep.* **2020**, *6*, 1973–1991. [\[CrossRef\]](#)
- International Energy Agency (IEA) and the World Bank. *Sustainable Energy for All 2017—Progress toward Sustainable Energy (Summary)*; Technical Report; License: Creative Commons Attribution CC BY 3.0 IGO; World Bank: Washington, DC, USA, 2017.
- Twaha, S.; Ramli, M.A. A review of optimization approaches for hybrid distributed energy generation systems: Off-grid and grid-connected systems. *Sustain. Cities Soc.* **2018**, *41*, 320–331. [\[CrossRef\]](#)
- Lian, J.; Zhang, Y.; Ma, C.; Yang, Y.; Chaima, E. A review on recent sizing methodologies of hybrid renewable energy systems. *Energy Convers. Manag.* **2019**, *199*, 112027. [\[CrossRef\]](#)
- Torres-Madroño, J.L.; Tamayo-Avenida, J.M.; Bernal-del Río, S.; Sierra-Pérez, J.; Nieto-Londoño, C.; Mejía-Gutiérrez, R.; Osorio-Gómez, G. Formulation and simulation of a hybrid solar PV-wind generation system with photovoltaic concentration for non-interconnected areas to the energy grid. *E3S Web Conf.* **2020**, *181*, 02002. [\[CrossRef\]](#)
- Torres-Madroño, J.L.; Nieto-Londoño, C.; Sierra-Pérez, J. Hybrid Energy Systems Sizing for the Colombian Context: A Genetic Algorithm and Particle Swarm Optimization Approach. *Energies* **2020**, *13*, 5648. [\[CrossRef\]](#)
- Moreno-Gamboa, F.; Escudero-Atehortúa, A.; Nieto-Londoño, C. Performance evaluation of external fired hybrid solar gas-turbine power plant in Colombia using energy and exergy methods. *Therm. Sci. Eng. Prog.* **2020**, *20*, 100679. [\[CrossRef\]](#)
- United Nations. *The Sustainable Development Goals Report 2020*; Technical Report; United Nations Publications: New York, NY, USA, 2020.
- Stoll, B.; Andrade, J.; Cohen, S.; Brinkman, G.; Martinez-Anido, C.B. *Hydropower Modeling Challenges*; Technical Report NREL/TP-5D00-68231; Prepared under Task No. WFGX.1040; National Renewable Energy Laboratory: Golden, CO, USA, 2017.
- Arango-Aramburo, S.; Turner, S.W.; Daenzer, K.; Ríos-Ocampo, J.P.; Hejazi, M.I.; Kober, T.; Álvarez-Espinosa, A.C.; Romero-Otalora, G.D.; van der Zwaan, B. Climate impacts on hydropower in Colombia: A multi-model assessment of power sector adaptation pathways. *Energy Policy* **2019**, *128*, 179–188. [\[CrossRef\]](#)
- Kondolf, G.M.; Gao, Y.; Annandale, G.W.; Morris, G.L.; Jiang, E.; Zhang, J.; Cao, Y.; Carling, P.; Fu, K.; Guo, Q.; et al. Sustainable sediment management in reservoirs and regulated rivers: Experiences from five continents. *Earth Future* **2014**, *2*, 256–280. [\[CrossRef\]](#)
- del Río, D.A.; Moffett, H.; Nieto-Londoño, C.; Vásquez, R.E.; Escudero-Atehortúa, A. Chivor’s Life Extension Project (CLEP): From Sediment Management to Development of a New Intake System. *Water* **2020**, *12*, 2743. [\[CrossRef\]](#)
- REN21. *Renewables 2018 Global Status Report. A Comprehensive Annual Overview of the State of Renewable Energy*; Technical Report GSR2018; REN21 Secretariat: Paris, France, 2018.

15. Jouhara, H.; Żabnieńska Góra, A.; Khordehgah, N.; Ahmad, D.; Lipinski, T. Latent Thermal Energy Storage Technologies and Applications: A Review. *Int. J. Thermofluids* **2020**, *2020*, 100039. [\[CrossRef\]](#)
16. Jouhara, H.; Khordehgah, N.; Almahmoud, S.; Delpech, B.; Chauhan, A.; Tassou, S.A. Waste heat recovery technologies and applications. *Therm. Sci. Eng. Prog.* **2018**, *6*, 268–289. [\[CrossRef\]](#)
17. Fierro, J.J.; Escudero-Atehortua, A.; Nieto-Londoño, C.; Giraldo, M.; Jouhara, H.; Wrobel, L.C. Evaluation of waste heat recovery technologies for the cement industry. *Int. J. Thermofluids* **2020**, *7–8*, 100040. [\[CrossRef\]](#)
18. WWEA: World Wind Energy Association. 2017 Summary: Small Wind World Repprt. Available online: <https://wwindea.org/blog/2017/06/02/wwea-released-latest-global-small-wind-statistics/> (accessed on 17 September 2020).
19. The International Renewable Energy Agency. *Quality Infrastructure for RETs—Small Wind Turbines (for Policy Makers)*; IRENA: Abu Dhabi, UAE, 2015; p. 56.
20. The International Renewable Energy Agency. IRENA. Wind power—Technology Brief. *Energy* **2016**, 1–24.
21. The International Renewable Energy Agency. IRENA. Renewable Energy Sources. Available online: <https://www.irena.org/> (accessed on 1 May 2019).
22. The International Renewable Energy Agency. IRENA. Wind Energy. Available online: <https://www.irena.org/wind> (accessed on 9 April 2020).
23. Moreira Chagas, C.C.; Pereira, M.G.; Rosa, L.P.; da Silva, N.F.; Vasconcelos Freitas, M.A.; Hunt, J.D. From megawatts to kilowatts: A review of small wind turbine applications, lessons from the US to Brazil. *Sustainability* **2020**, *12*, 2760. [\[CrossRef\]](#)
24. Small Wind Certification Council. *ICC-SWCC Summary Report SWCC-11-04*; Technical Report; Small Wind Certification Council: Brea, CA, USA, 2019.
25. Small Wind Certification Council. *ICC-SWCC Summary Report SWCC-10-12*; Technical Report; Small Wind Certification Council: Brea, CA, USA, 2019.
26. Small Wind Certification Council. *ICC-SWCC SUMMARY REPORT LPP-16-05*; Technical Report; Small Wind Certification Council: Brea, CA, USA, 2019.
27. Leary, J.; Czyrnek-Delètre, M.; Alsop, A.; Eales, A.; Marandin, L.; Org, M.; Craig, M.; Ortiz, W.; Casillas, C.; Persson, J.; et al. Finding the niche: A review of market assessment methodologies for rural electrification with small scale wind power. *Renew. Sustain. Energy Rev.* **2020**, *133*, 110240. [\[CrossRef\]](#)
28. El-Askary, W.A.; Sakr, I.M.; AbdelSalam, A.M.; Abuhegazy, M.R. Modeling of wind turbine wakes under thermally-stratified atmospheric boundary layer. *J. Wind. Eng. Ind. Aerodyn.* **2017**, *160*, 1–15. [\[CrossRef\]](#)
29. Battisti, L.; Benini, E.; Brighenti, A.; Dell’Anna, S.; Raciti Castelli, M. Small wind turbine effectiveness in the urban environment. *Renew. Energy* **2018**, *129*, 102–113. [\[CrossRef\]](#)
30. Tabassum, M.; Kashem, S.B.A.; Mathew, K. Distributed energy generation—Is it the way of the future? *Lect. Notes Electr. Eng.* **2018**, *436*, 627–636. [\[CrossRef\]](#)
31. Tummala, A.; Velamati, R.K.; Sinha, D.K.; Indraj, V.; Krishna, V.H. A review on small scale wind turbines. *Renew. Sustain. Energy Rev.* **2016**, *56*, 1351–1371. [\[CrossRef\]](#)
32. Nolan Clark, R. *Small Wind: Planning and Building Successful Installations*; Cambridge University Press: Cambridge, UK, 2014. [\[CrossRef\]](#)
33. Jurasz, J.; Canales, F.A.; Kies, A.; Guezgouz, M.; Beluco, A. A review on the complementarity of renewable energy sources: Concept, metrics, application and future research directions. *Renew. Sustain. Energy Rev.* **2019**, *195*, 703–724. [\[CrossRef\]](#)
34. Tadie Fogaing, M.B.; Gordon, H.; Lange, C.F.; Wood, D.H.; Fleck, B.A. A Review of Wind Energy Resource Assessment in the Urban Environment. *Lect. Notes Energy* **2019**, *70*, 7–36. [\[CrossRef\]](#)
35. James, P.A.B.; Bahaj, A.S. *Small-Scale Wind Turbines*; Elsevier Inc.: Cambridge, MA, USA, 2017; pp. 389–418. [\[CrossRef\]](#)
36. Micallef, D.; Van Bussel, G. A review of urban wind energy research: Aerodynamics and other challenges. *Energies* **2018**, *11*, 2204. [\[CrossRef\]](#)
37. KC, A.; Whale, J.; Urmee, T. Urban wind conditions and small wind turbines in the built environment: A review. *Renew. Energy* **2019**, *131*, 268–283. [\[CrossRef\]](#)

38. Karthikeyan, N.; Kalidas Murugavel, K.; Arun Kumar, S.; Rajakumar, S. Review of aerodynamic developments on small horizontal axis wind turbine blade. *Renew. Sustain. Energy Rev.* **2015**, *42*, 801–822. [\[CrossRef\]](#)
39. Menezes, E.J.N.; Araújo, A.M.; da Silva, N.S.B. A review on wind turbine control and its associated methods. *J. Clean. Prod.* **2018**, *174*, 945–953. [\[CrossRef\]](#)
40. Murthy, K.; Rahi, O. A comprehensive review of wind resource assessment. *Renew. Sustain. Energy Rev.* **2017**, *72*, 1320–1342. [\[CrossRef\]](#)
41. Krohn, S.; Morthorst, P.E.; Awerbuch, S. The economics of wind energy. *Eur. Wind. Energy Assoc.* **2009**, *13*, 28–29.
42. Elsner, P.; Suarez, S. Renewable energy from the high seas: Geo-spatial modelling of resource potential and legal implications for developing offshore wind projects beyond the national jurisdiction of coastal States. *Energy Policy* **2019**, *128*, 919–929. [\[CrossRef\]](#)
43. Tandjaoui, M.; Benachaiba, C.; Abdelkhalek, O.; Dennai, B.; Mouloudi, Y. The Impact of Wind Power Implantation in Transmission Systems. *Energy Procedia* **2013**, *36*, 260–267. [\[CrossRef\]](#)
44. Oke, T.R. *Boundary Layer Climates*, 2nd ed.; Routledge: London, UK, 1987.
45. Abohela, I.; Hamza, N.; Dudek, S. Effect of roof shape, wind direction, building height and urban configuration on the energy yield and positioning of roof mounted wind turbines. *Renew. Energy* **2013**, *50*, 1106–1118. [\[CrossRef\]](#)
46. Mannan, S. (Ed.) Chapter 15—Emission and Dispersion. In *Lees' Loss Prevention in the Process Industries (Fourth Edition)*, 4th ed.; Butterworth-Heinemann: Oxford, UK, 2012; pp. 752–1074. [\[CrossRef\]](#)
47. ABB. *Cuaderno de Aplicaciones Técnicas. Plantas Eólicas*; ABB: Barcelona, Spain, 2010; pp. 1–109.
48. Masseran, N. Markov Chain model for the stochastic behaviors of wind-direction data. *Energy Convers. Manag.* **2015**, *92*, 266–274. [\[CrossRef\]](#)
49. Acosta, J.L.; Combe, K.; Djokić, S.Ž.; Hernando-Gil, I. Performance assessment of micro and small-scale wind turbines in urban areas. *IEEE Syst. J.* **2012**, *6*, 152–163. [\[CrossRef\]](#)
50. Sedaghat, A.; Hassanzadeh, A.; Jamali, J.; Mostafaiepour, A.; Chen, W.H. Determination of rated wind speed for maximum annual energy production of variable speed wind turbines. *Appl. Energy* **2017**, *205*, 781–789. [\[CrossRef\]](#)
51. IEC. IEC 61400-2. *Wind Turbines—Part 2: Small Wind Turbines*; IEC: Geneva, Switzerland, 2013.
52. Zhou, Q.; Wang, C.; Zhang, G. Hybrid forecasting system based on an optimal model selection strategy for different wind speed forecasting problems. *Appl. Energy* **2019**, *250*, 1559–1580. [\[CrossRef\]](#)
53. Toja-Silva, F.; Kono, T.; Peralta, C.; Lopez-Garcia, O.; Chen, J. A review of computational fluid dynamics (CFD) simulations of the wind flow around buildings for urban wind energy exploitation. *J. Wind. Eng. Ind. Aerodyn.* **2018**, *180*, 66–87. [\[CrossRef\]](#)
54. Toja-Silva, F.; Peralta, C.; Lopez-Garcia, O.; Navarro, J.; Cruz, I. Roof region dependent wind potential assessment with different RANS turbulence models. *J. Wind. Eng. Ind. Aerodyn.* **2015**, *142*, 258–271. [\[CrossRef\]](#)
55. Antoniou, N.; Montazeri, H.; Neophytou, M.; Blocken, B. CFD simulation of urban microclimate: Validation using high-resolution field measurements. *Sci. Total Environ.* **2019**, *695*. [\[CrossRef\]](#)
56. Argyropoulos, C.D.; Markatos, N.C. Recent advances on the numerical modelling of turbulent flows. *Appl. Math. Model.* **2015**, *39*, 693–732. [\[CrossRef\]](#)
57. Nieto, F.; Hargreaves, D.M.; Owen, J.S.; Hernández, S. On the applicability of 2D URANS and SST k- $\omega$  turbulence model to the fluid-structure interaction of rectangular cylinders. *Eng. Appl. Comput. Fluid Mech.* **2015**, *9*, 157–173. [\[CrossRef\]](#)
58. Markatos, N.C. The mathematical modelling of turbulent flows. *Appl. Math. Model.* **1986**, *10*, 190–220. [\[CrossRef\]](#)
59. Toja-Silva, F.; Peralta, C.; Lopez-Garcia, O.; Navarro, J.; Cruz, I. On roof geometry for urban wind energy exploitation in high-rise buildings. *Computation* **2015**, *3*, 299–325. [\[CrossRef\]](#)
60. Rakib, M.I.; Evans, S.P.; Clausen, P.D. Measured gust events in the urban environment, a comparison with the IEC standard. *Renew. Energy* **2020**, *146*, 1134–1142. [\[CrossRef\]](#)
61. Davis, F.K.; Newstein, H. The Variation of Gust Factors with Mean Wind Speed and with Height. *J. Appl. Meteorol.* **1968**, *7*, 372–378. [\[CrossRef\]](#)

62. Antonio, O.L.C.; Wood, D.H. Measurements of semi-urban gust factors for wind load determination. *Green Energy Technol.* **2018**, *PartF10*, 17–25. [\[CrossRef\]](#)
63. KC, A.; Whale, J.; Evans, S.P.; Clausen, P.D. An investigation of the impact of wind speed and turbulence on small wind turbine operation and fatigue loads. *Renew. Energy* **2020**, *146*, 87–98. [\[CrossRef\]](#)
64. Woolmington, T.; Sunderland, K.; Blackledge, J.; Conlon, M. The progressive development of turbulence statistics and its impact on wind power predictability. *Energy* **2014**, *77*, 25–34. [\[CrossRef\]](#)
65. Rakib, M.I.; Nay, S.; Evans, S.; Clausen, P. Wind Regimes in Urban Environments: Experimental Comparison with the IEC 61400.2-2013 Open Terrain Wind Model. *Res. Top. Wind. Energy* **2019**, *8*, 201–214. [\[CrossRef\]](#)
66. Dilimulati, A.; Stathopoulos, T.; Paraschivoiu, M. Wind turbine designs for urban applications: A case study of shrouded diffuser casing for turbines. *J. Wind. Eng. Ind. Aerodyn.* **2018**, *175*, 179–192. [\[CrossRef\]](#)
67. Pagnini, L.C.; Burlando, M.; Repetto, M.P. Experimental power curve of small-size wind turbines in turbulent urban environment. *Appl. Energy* **2015**, *154*, 112–121. [\[CrossRef\]](#)
68. Lubitz, W.D. Impact of ambient turbulence on performance of a small wind turbine. *Renew. Energy* **2014**, *61*, 69–73. [\[CrossRef\]](#)
69. Ward, N.J.; Stewart, S.W. A turbulence intensity similarity distribution for evaluating the performance of a small wind turbine in turbulent wind regimes. *Wind Eng.* **2015**, *39*, 661–673. [\[CrossRef\]](#)
70. Cooney, C.; Byrne, R.; Lyons, W.; O'Rourke, F. Performance characterisation of a commercial-scale wind turbine operating in an urban environment, using real data. *Energy Sustain. Dev.* **2017**, *36*, 44–54. [\[CrossRef\]](#)
71. Carbó Molina, A.; De Troyer, T.; Massai, T.; Vergaerde, A.; Runacres, M.C.; Bartoli, G. Effect of turbulence on the performance of VAWTs: An experimental study in two different wind tunnels. *J. Wind. Eng. Ind. Aerodyn.* **2019**, *193*. [\[CrossRef\]](#)
72. Emejeamara, F.C.; Tomlin, A.S. A method for estimating the potential power available to building mounted wind turbines within turbulent urban air flows. *Renew. Energy* **2020**, *153*, 787–800. [\[CrossRef\]](#)
73. Emejeamara, F.C.; Tomlin, A.S.; Millward-Hopkins, J.T. Urban wind: Characterisation of useful gust and energy capture. *Renew. Energy* **2015**, *81*, 162–172. [\[CrossRef\]](#)
74. Orrell, A.; Preziuso, D.; Foster, N.; Morris, S.; Homer, J. *2018 Distributed Wind Market Report*; Technical Report; USDOE Office of Energy Efficiency and Renewable Energy: Richland, WA, USA, 2019.
75. IRENA Secretariat. *Renewable Energy Technologies: Cost Analysis Series, Wind Power*; Technical Report; International Renewable Energy Agency (IRENA): Abu Dhabi, UAE, 2012.
76. Tangler, J.L.; Somers, D.M. *NREL Airfoil Families for HAWTs*; Technical Report; National Renewable Energy Laboratory: Golden, CO, USA, 1995.
77. Somers, D.M. *The S825 and S826 Airfoils*; Technical Report; National Renewable Energy Laboratory: Golden, CO, USA, 2005.
78. Somers, D.M. *The S822 and S823 Airfoils*. Technical Report; National Renewable Energy Laboratory: Golden, CO, USA, 2005.
79. Somers, D.M. *The S833, S834, and S835 Airfoils*; Technical Report; National Renewable Energy Laboratory: Golden, CO, USA, 2005. [\[CrossRef\]](#)
80. Giguère, P.; Selig, M.S. New airfoils for small horizontal axis wind turbines. *J. Sol. Energy Eng. Trans. ASME* **1998**, *120*, 108–114. [\[CrossRef\]](#)
81. Tangler, J. *The Evolution of Rotor and Blade Design*; Technical Report; National Renewable Energy Lab.: Golden, CO, USA, 2000.
82. Lissaman, P.B.S. Low-reynolds-number airfoils. *Annu. Rev. Fluid Mech.* **1983**, *15*, 223–239. [\[CrossRef\]](#)
83. Selig, M.; McGranahan, B. Wind tunnel aerodynamic tests of six airfoils for use on small wind turbines. In Proceedings of the 42nd AIAA Aerospace Sciences Meeting and Exhibit, Reno, NV, USA, 5–8 January 2004; p. 1188.
84. Selig, M.S.; Guglielmo, J.; Broeren, A.; Guigère, P. *Summary of Low-Speed Airfoil Data Vol. 1*; SoarTech Publications: Virginia Beach, WV, USA, 1995.
85. Selig, M.S.; Lyon, C.A.; Giguere, P.; Ninham, C.P.; Guglielmo, J.J. *Summary of Low-Speed Airfoil Data Vol. 2*; SoarTech Publications: Virginia Beach, WV, USA, 1996.



86. Lyon, C.A.; Broeren, A.P.; Guigère, P.; Gopalarathnam, A.; Selig, M.S. *Summary of Low-Speed Airfoil Data Vol. 3*; SoarTech Publications: Virginia Beach, WV, USA, 1997.
87. Henriques, J.C.; Marques da Silva, F.; Estanqueiro, A.I.; Gato, L.M. Design of a new urban wind turbine airfoil using a pressure-load inverse method. *Renew. Energy* **2009**, *34*, 2728–2734. [[CrossRef](#)]
88. Kim, T.; Lee, S.; Kim, H.; Lee, S. Design of low noise airfoil with high aerodynamic performance for use on small wind turbines. *Sci. China Technol. Sci.* **2010**, *53*, 75–79. [[CrossRef](#)]
89. Drela, M. XFOIL: An Analysis and Design System for Low Reynolds Number Airfoils. In *Low Reynolds Number Aerodynamics*; Mueller, T.J., Ed.; Springer: Berlin/Heidelberg, Germany, 1989; pp. 1–12.
90. Natarajan, K.; Thomas, S.; Ramachadran Bhagavathi Ammal, A. Numerical Investigation of Airfoils For Small Wind Turbine Applications. *Therm. Sci.* **2016**, *20*, S1091–S1098. [[CrossRef](#)]
91. Van Treuren, K.W. Small-Scale Wind Turbine Testing in Wind Tunnels Under Low Reynolds Number Conditions. *J. Energy Resour. Technol. Trans. ASME* **2015**, *137*, 051208. [[CrossRef](#)]
92. Grasso, F. Usage of numerical optimization in wind turbine airfoil design. *J. Aircr.* **2011**, *48*, 248–255. [[CrossRef](#)]
93. Grasso, F. Hybrid optimization for wind turbine thick airfoils. In Proceedings of the 53rd AIAA/ASME/ASCE/AHS/ASC Structures, Structural Dynamics and Materials Conference, Honolulu, HI, USA, 23–26 April 2012; pp. 1–12.
94. Benim, A.C.; Diederich, M.; Pfeiffelmann, B. Aerodynamic optimization of airfoil profiles for small horizontal axis wind turbines. *Computation* **2018**, *6*, 34. [[CrossRef](#)]
95. Ram, K.R.; Lal, S.; Rafiuddin Ahmed, M. Low Reynolds number airfoil optimization for wind turbine applications using genetic algorithm. *J. Renew. Sustain. Energy* **2013**, *5*. [[CrossRef](#)]
96. Wata, J.; Faizal, M.; Talu, B.; Vanawalu, L.; Sotia, P.; Ahmed, M.R. Studies on a low Reynolds number airfoil for small wind turbine applications. *Sci. China Technol. Sci.* **2011**, *54*, 1684–1688. [[CrossRef](#)]
97. Singh, R.K.; Ahmed, M.R.; Zullah, M.A.; Lee, Y.H. Design of a low Reynolds number airfoil for small horizontal axis wind turbines. *Renew. Energy* **2012**, *42*, 66–76. [[CrossRef](#)]
98. Hall, D.R. Airfoil Designs for a Small and Large Horizontal Axis Wind Turbine. In Proceedings of the 53rd AIAA Aerospace Sciences Meeting, Kissimmee, FL, USA, 5–9 January 2015; p. 1034.
99. Chillon, S.; Uriarte-Uriarte, A.; Aramendia, I.; Martínez-Filgueira, P.; Fernandez-Gamiz, U.; Ibarra-Udaeta, I. jBAY Modeling of Vane-Type Vortex Generators and Study on Airfoil Aerodynamic Performance. *Energies* **2020**, *13*, 2423. [[CrossRef](#)]
100. Hutchinson, J.; Schubel, P.; Warrior, N. A cost and performance comparison of LRTM and VI for the manufacture of large scale wind turbine blades. *Renew. Energy* **2011**, *36*, 866–871. [[CrossRef](#)]
101. Melendez-Vega, P.A.; Venkataramanan, G.; Ludois, D.; Reed, J. Low-Cost Light-Weight Quick-Manufacturable Blades for Human-Scale Wind Turbines. In Proceedings of the 2011 IEEE Global Humanitarian Technology Conference, Seattle, WA, USA, 30 October–1 November 2011; pp. 154–159. [[CrossRef](#)]
102. Latoufis, K.; Pazios, T.; Hatzigiorgiou, N. Locally Manufactured Small Wind Turbines: Empowering communities for sustainable rural electrification. *IEEE Electr. Mag.* **2015**, *3*, 68–78. [[CrossRef](#)]
103. Pourrajabian, A.; Dehghan, M.; Javed, A.; Wood, D. Choosing an appropriate timber for a small wind turbine blade: A comparative study. *Renew. Sustain. Energy Rev.* **2019**, *100*, 1–8. [[CrossRef](#)]
104. Clausen, P.D.; Reynal, F.; Wood, D.H.; Reynal, F.; Wood, D.H. Design, manufacture and testing of small wind turbine blades. In *Advances in Wind Turbine Blade Design and Materials*; Elsevier: Cambridge, UK, 2013; pp. 413–431. [[CrossRef](#)]
105. Latoufis, K.; Riziotis, V.; Voutsinas, S.; Hatzigiorgiou, N. Effects of Leading Edge Erosion on the Power Performance and Acoustic Noise Emissions of Locally Manufactured Small Wind Turbine Blades. *J. Phys. Conf. Ser.* **2019**, *1222*, 012010. [[CrossRef](#)]
106. Wood, D. Small Wind Turbines. In *Green Energy and Technology*; Springer: London, UK, 2011. [[CrossRef](#)]
107. Mishnaevsky, L.; Branner, K.; Petersen, H.N.; Beauson, J.; McGugan, M.; Sørensen, B.F.; Mishnaevsky, L., Jr.; Branner, K.; Petersen, H.N.; Beauson, J.; et al. Materials for wind turbine blades: An overview. *Materials* **2017**, *10*, 1285. [[CrossRef](#)] [[PubMed](#)]



108. Sharma, S.; Wetzel, K.K. Process Development Issues of Glass—Carbon Hybrid-reinforced Polymer Composite Wind Turbine Blades. *J. Compos. Mater.* **2010**, *44*, 437–456. [\[CrossRef\]](#)
109. Lawrence, J.M.; Neacsu, V.; Advani, S.G. Modeling the impact of capillary pressure and air entrapment on fiber tow saturation during resin infusion in LCM. *Compos. Part A Appl. Sci. Manuf.* **2009**, *40*, 1053–1064. [\[CrossRef\]](#)
110. van Oosterom, S.; Allen, T.; Battley, M.; Bickerton, S. An objective comparison of common vacuum assisted resin infusion processes. *Compos. Part A Appl. Sci. Manuf.* **2019**, *125*, 105528. [\[CrossRef\]](#)
111. Patiño, I.D.; Power, H.; Nieto-Londoño, C.; Flórez, W.F. Stokes—Brinkman formulation for prediction of void formation in dual-scale fibrous reinforcements: A BEM/DR-BEM simulation. *Comput. Mech.* **2017**, *59*, 555–577. [\[CrossRef\]](#)
112. Patiño Arcila, I.; Power, H.; Nieto-Londoño, C.; Flórez Escobar, W. Boundary Element Method for the dynamic evolution of intra-tow voids in dual-scale fibrous reinforcements using a Stokes–Darcy formulation. *Eng. Anal. Bound. Elem.* **2018**, *87*, 133–152. [\[CrossRef\]](#)
113. Herrera, C.; Sierra-Pérez, J.; Nieto-Londoño, C. Analytical determination of viscous permeability of hybrid fibrous reinforcements. *Int. J. Thermofluids* **2020**, *7–8*, 100042. [\[CrossRef\]](#)
114. Correa-Álvarez, M.; Villada-Quiceno, V.; Sierra-Pérez, J.; García-Navarro, J.G.; Nieto-Londoño, C. Structural design of carbon/epoxy bio-inspired wind turbine blade using fluid/structure simulation. *Int. J. Energy Res.* **2016**, *40*, 1832–1845. [\[CrossRef\]](#)
115. Herrera, C.; Correa, M.; Villada, V.; Vanegas, J.; García, J.; Nieto-Londoño, C.; Sierra-Pérez, J. Structural design and manufacturing process of a low scale bio-inspired wind turbine blades. *Compos. Struct.* **2019**, *208*, 1–12. [\[CrossRef\]](#)
116. Kaminski, M.; Loth, E.; Griffith, D.T.; Qin, C.C. Ground testing of a 1additively-manufactured wind turbine blade with bio-inspired structural design. *Renew. Energy* **2020**, *148*, 639–650. [\[CrossRef\]](#)
117. Ikeda, T.; Tanaka, H.; Yoshimura, R.; Noda, R.; Fujii, T.; Liu, H. A robust biomimetic blade design for micro wind turbines. *Renew. Energy* **2018**, *125*, 155–165. [\[CrossRef\]](#)
118. Ng, B.; New, T.; Palacios, R. *Bio-Inspired Leading-Edge Tubercles to Improve Fatigue Life in Horizontal Axis Wind Turbine Blades*; American Institute of Aeronautics and Astronautics Inc., AIAA: Grapevine, TX, USA, 2017. [\[CrossRef\]](#)
119. Seidel, C.; Jayaram, S.; Kunkel, L.; Mackowski, A. Structural analysis of biologically inspired small wind turbine blades. *Int. J. Mech. Mater. Eng.* **2017**, *12*. [\[CrossRef\]](#)
120. Cognet, V.; Courrech du Pont, S.; Thiria, B. Material optimization of flexible blades for wind turbines. *Renew. Energy* **2020**, *160*, 1373–1384. [\[CrossRef\]](#)
121. Watson, S.; Moro, A.; Reis, V.; Baniotopoulos, C.; Barth, S.; Bartoli, G.; Bauer, F.; Boelman, E.; Bosse, D.; Cherubini, A.; et al. Future emerging technologies in the wind power sector: A European perspective. *Renew. Sustain. Energy Rev.* **2019**, *113*, 109270. [\[CrossRef\]](#)
122. Sessarego, M.; Wood, D. Multi-dimensional optimization of small wind turbine blades. *Renew. Wind Water Sol.* **2015**, *2*, 9. [\[CrossRef\]](#)
123. Poole, S.; Phillips, R. Rapid prototyping of small wind turbine blades using additive manufacturing. In Proceedings of the 2015 Pattern Recognition Association of South Africa and Robotics and Mechatronics International Conference (PRASA-RobMech), Port Elizabeth, South Africa, 26–27 November 2015; pp. 189–194. [\[CrossRef\]](#)
124. Chaudhary, M.; Prakash, S. Design and fabrication of small horizontal axis wind turbine rotors at low reynolds number. *Int. J. Innov. Technol. Explor. Eng.* **2019**, *8*, 4454–4463. [\[CrossRef\]](#)
125. Rahimizadeh, A.; Kalman, J.; Fayazbakhsh, K.; Lessard, L. Recycling of fiberglass wind turbine blades into reinforced filaments for use in Additive Manufacturing. *Compos. Part B Eng.* **2019**, *175*. [\[CrossRef\]](#)
126. Shah, D.U.; Schubel, P.J.; Clifford, M.J. Can flax replace E-glass in structural composites? A small wind turbine blade case study. *Compos. Part B Eng.* **2013**, *52*, 172–181. [\[CrossRef\]](#)
127. Sant, T.; Farrugia, R.N.; Muscat, M.; Caruana, C.; Axisa, R.; Borg, A.; Cassar, C.M.; Cassar, J.; Cordina, C.; Farrugia, A.; et al. Development and performance testing of a small, multi-bladed wind turbine. *Wind Eng.* **2019**. [\[CrossRef\]](#)

128. Bostan, V.; Bostan, I.; Dulgheru, V.; Sobor, I.; Vaculenco, M.; Odainai, V.; Gladis, V. Study of the aerodynamics of wind rotors with horizontal axis: Design, manufacture, testing. In Proceedings of the 2017 International Conference on Electromechanical and Power Systems (SIELMEN), Iasi, Romania, 11–13 October 2017; pp. 308–314. [\[CrossRef\]](#)
129. Kam, T.Y. Design and Fabrication of Composite Wind Blades for a 5kW Wind Power System. In *ASME International Mechanical Engineering Congress and Exposition*; American Society of Mechanical Engineers: New York, NY, USA, 2012; Volume 3, pp. 513–518. [\[CrossRef\]](#)
130. Xie, W.; Zeng, P.; Lei, L. A novel folding blade of wind turbine rotor for effective power control. *Energy Convers. Manag.* **2015**, *101*, 52–65. [\[CrossRef\]](#)
131. Xie, W.; Zeng, P.; Lei, L. Wind tunnel experiments for innovative pitch regulated blade of horizontal axis wind turbine. *Energy* **2015**, *91*, 1070–1080. [\[CrossRef\]](#)
132. Hatami, A.; Moetakef-Imani, B. Innovative adaptive pitch control for small wind turbine fatigue load reduction. *Mechatronics* **2016**, *40*, 137–145. [\[CrossRef\]](#)
133. Rocha, P.C.; de Araujo, J.C.; Lima, R.P.; da Silva, M.V.; Albiero, D.; de Andrade, C.; Carneiro, F. The effects of blade pitch angle on the performance of small-scale wind turbine in urban environments. *Energy* **2018**, *148*, 169–178. [\[CrossRef\]](#)
134. Mohammadi, E.; Fadaeinedjad, R.; Naji, H.R. Flicker emission, voltage fluctuations, and mechanical loads for small-scale stall- and yaw-controlled wind turbines. *Energy Convers. Manag.* **2018**, *165*, 567–577. [\[CrossRef\]](#)
135. Civelek, Z. Optimization of fuzzy logic (Takagi-Sugeno) blade pitch angle controller in wind turbines by genetic algorithm. *Eng. Sci. Technol. Int. J.* **2019**. [\[CrossRef\]](#)
136. Khaled, M.; Ibrahim, M.M.; Hamed, H.E.A.; AbdelGwad, A.F. Investigation of a small Horizontal-Axis wind turbine performance with and without winglet. *Energy* **2019**, *187*, 115921. [\[CrossRef\]](#)
137. Venkaiah, P.; Sarkar, B.K. Hydraulically actuated horizontal axis wind turbine pitch control by model free adaptive controller. *Renew. Energy* **2020**, *147*, 55–68. [\[CrossRef\]](#)
138. Siavash, N.K.; Najafi, G.; Hashjin, T.T.; Ghobadian, B.; Mahmoodi, E. An innovative variable shroud for micro wind turbines. *Renew. Energy* **2020**, *145*, 1061–1072. [\[CrossRef\]](#)
139. Jukes, T.N. Smart control of a horizontal axis wind turbine using dielectric barrier discharge plasma actuators. *Renew. Energy* **2015**, *80*, 644–654. [\[CrossRef\]](#)
140. Maheri, A.; Noroozi, S.; Toomer, C.; Vinney, J. A simple algorithm to modify an ordinary wind turbine blade to an adaptive one. In Proceedings of the European Wind Energy Conference, Athens, Greece, 27 February–2 March 2006; Volume 2, pp. 1195–1202.
141. Nicholls-Lee, R.F.; Turnock, S.R. Enhancing performance of a horizontal axis tidal turbine using adaptive blades. In Proceedings of the OCEANS 2007-Europe, Aberdeen, Scotland, 18–21 June 2007. [\[CrossRef\]](#)
142. Barr, S.M.; Jaworski, J.W. Optimization of tow-steered composite wind turbine blades for static aeroelastic performance. *Renew. Energy* **2019**, *139*, 859–872. [\[CrossRef\]](#)
143. Capuzzi, M.; Pirrera, A.; Weaver, P.M. A novel adaptive blade concept for large-scale wind turbines. Part I: Aeroelastic behaviour. *Energy* **2014**, *73*, 15–24. [\[CrossRef\]](#)
144. Capuzzi, M.; Pirrera, A.; Weaver, P.M. A novel adaptive blade concept for large-scale wind turbines. Part II: Structural design and power performance. *Energy* **2014**, *73*, 25–32. [\[CrossRef\]](#)
145. Capuzzi, M.; Pirrera, A.; Weaver, P.M. Structural design of a novel aeroelastically tailored wind turbine blade. *Thin-Walled Struct.* **2015**, *95*, 7–15. [\[CrossRef\]](#)
146. Zahle, F.; Tibaldi, C.; Pavese, C.; McWilliam, M.K.; Blasques, J.; Hansen, M.H. Design of an Aeroelastically Tailored 10 MW Wind Turbine Rotor. *J. Phys. Conf. Ser.* **2016**, *753*. [\[CrossRef\]](#)
147. Restrepo-Montoya, D.; Alvarez-Montoya, J.; Sierra-Pérez, J.; Nieto-Londoño, C. Artificial Intelligence Metamodeling Approach to Design Smart Composite Laminates with Bend-Twist Coupling. In Proceedings of the 2019 IEEE 2nd International Conference on Renewable Energy and Power Engineering (REPE), Toronto, ON, Canada, 2–4 November 2019; pp. 155–159.
148. Herath, M.T.; Lee, A.K.L.; Prusty, B.G. Design of shape-adaptive wind turbine blades using Differential Stiffness Bend-Twist coupling. *Ocean Eng.* **2015**, *95*, 157–165. [\[CrossRef\]](#)

149. Maheri, A.; Noroozi, S.; Vinney, J. Application of combined analytical/FEA coupled aero-structure simulation in design of wind turbine adaptive blades. *Renew. Energy* **2007**, *32*, 2011–2018. [\[CrossRef\]](#)
150. Vesel, R.W.; McNamara, J.J. Performance enhancement and load reduction of a 5MW wind turbine blade. *Renew. Energy* **2014**, *66*, 391–401. [\[CrossRef\]](#)
151. Scott, S.; Capuzzi, M.; Langston, D.; Bossanyi, E.; McCann, G.; Weaver, P.M.; Pirrera, A. Effects of aeroelastic tailoring on performance characteristics of wind turbine systems. *Renew. Energy* **2017**, *114*, 887–903. [\[CrossRef\]](#)
152. Bianchini, A.; Ferrara, G.; Ferrari, L. Pitch Optimization in Small-size Darrieus Wind Turbines. *Energy Procedia* **2015**, *81*, 122–132. [\[CrossRef\]](#)
153. Abdalrahman, G.; Melek, W.; Lien, F.S. Pitch angle control for a small-scale Darrieus vertical axis wind turbine with straight blades (H-Type VAWT). *Renew. Energy* **2017**, *114*, 1353–1362. [\[CrossRef\]](#)
154. Sagharichi, A.; Ghaghelestani, T.N.; Toudarbari, S. Impact of harmonic pitch functions on performance of Darrieus wind turbine. *J. Clean. Prod.* **2019**, *241*, 118310. [\[CrossRef\]](#)
155. de Boer, H.S.H.S.; van Vuuren, D.D.P. Representation of variable renewable energy sources in TIMER, an aggregated energy system simulation model. *Energy Econ.* **2017**, *64*, 600–611. [\[CrossRef\]](#)
156. Abbes, D.; Martinez, A.; Champenois, G. Life cycle cost, embodied energy and loss of power supply probability for the optimal design of hybrid power systems. *Math. Comput. Simul.* **2014**, *98*, 46–62. [\[CrossRef\]](#)
157. Impram, S.; Varbak Nese, S.; Oral, B. Challenges of renewable energy penetration on power system flexibility: A survey. *Energy Strategy Rev.* **2020**, *31*, 100539. [\[CrossRef\]](#)
158. Paredes, J.R.; Ramírez, J.J. *Variable Renewable Energies and Their Contribution to Energy Security: Complementarity in Colombia*; Banco Interamericano de Desarrollo: Washington, DC, USA, 2017; p. 59.
159. Bhandari, B.; Poudel, S.R.; Lee, K.T.; Ahn, S.H. Mathematical modeling of hybrid renewable energy system: A review on small hydro-solar-wind power generation. *Int. J. Precis. Eng. Manuf. Green Technol.* **2014**, *1*, 157–173. [\[CrossRef\]](#)
160. Koutroulis, E.; Kolokotsa, D.; Potirakis, A.; Kalaitzakis, K. Methodology for optimal sizing of stand-alone photovoltaic/wind-generator systems using genetic algorithms. *Sol. Energy* **2006**, *80*, 1072–1088. [\[CrossRef\]](#)
161. Lehtola, T.; Zahedi, A. Solar energy and wind power supply supported by storage technology: A review. *Sustain. Energy Technol. Assess.* **2019**, *35*, 25–31. [\[CrossRef\]](#)
162. Huu, D.N. An innovative adaptive droop control based on available energy for dc micro distribution grids y. *Energies* **2020**, *13*, 2983. [\[CrossRef\]](#)
163. Mahesh, A.; Sandhu, K.S. Hybrid wind/photovoltaic energy system developments: Critical review and findings. *Renew. Sustain. Energy Rev.* **2015**, *52*, 1135–1147. [\[CrossRef\]](#)
164. Shivarama Krishna, K.; Sathish Kumar, K. A review on hybrid renewable energy systems. *Renew. Sustain. Energy Rev.* **2015**, *52*, 907–916. [\[CrossRef\]](#)
165. Chauhan, A.; Saini, R.P. A review on Integrated Renewable Energy System based power generation for stand-alone applications: Configurations, storage options, sizing methodologies and control. *Renew. Sustain. Energy Rev.* **2014**, *38*, 99–120. [\[CrossRef\]](#)
166. Siddaiah, R.; Saini, R.P. A review on planning, configurations, modeling and optimization techniques of hybrid renewable energy systems for off grid applications. *Renew. Sustain. Energy Rev.* **2016**, *58*, 376–396. [\[CrossRef\]](#)
167. Tezer, T.; Yaman, R.; Yaman, G. Evaluation of approaches used for optimization of stand-alone hybrid renewable energy systems. *Renew. Sustain. Energy Rev.* **2017**, *73*, 840–853. [\[CrossRef\]](#)
168. Kajela, D.; Manshahia, M.S. Optimization of Renewable Energy Systems: A Review. *Int. J. Sci. Res. Sci. Technol.* **2017**, *3*, 769–794. [\[CrossRef\]](#)
169. Chaib, A.; Achour, D.; Kesraoui, M. Control of a Solar PV/wind Hybrid Energy System. *Energy Procedia* **2016**, *95*, 89–97. [\[CrossRef\]](#)
170. Sinha, S.; Chandel, S.S. Review of recent trends in optimization techniques for solar photovoltaic-wind based hybrid energy systems. *Renew. Sustain. Energy Rev.* **2015**, *50*, 755–769. [\[CrossRef\]](#)
171. Khare, V.; Nema, S.; Baredar, P. Solar-wind hybrid renewable energy system: A review. *Renew. Sustain. Energy Rev.* **2016**, *58*, 23–33. [\[CrossRef\]](#)

172. Al-falahi, M.D.; Jayasinghe, S.D.; Enshaei, H. A review on recent size optimization methodologies for standalone solar and wind hybrid renewable energy system. *Energy Convers. Manag.* **2017**, *143*, 252–274. [CrossRef]
173. Maleki, A.; Pourfayaz, F. Optimal sizing of autonomous hybrid photovoltaic/wind/battery power system with LPSP technology by using evolutionary algorithms. *Sol. Energy* **2015**, *115*, 471–483. [CrossRef]
174. Mayer, M.J.; Szilágyi, A.; Gróf, G. Environmental and economic multi-objective optimization of a household level hybrid renewable energy system by genetic algorithm. *Appl. Energy* **2020**, *269*, 115058. [CrossRef]
175. Erich, H. *Wind Turbines: Fundamentals, Technologies, Application, Economics*; Springer: Berlin/Heidelberg, Germany, 2006.
176. Abdelhady, S.; Borello, D.; Santori, S. Economic Feasibility of Small Wind Turbines for Domestic Consumers in Egypt Based on the New Feed-in Tariff. *Energy Procedia* **2015**, *75*, 664–670. [CrossRef]
177. Rodriguez-Hernandez, O.; Martinez, M.; Lopez-Villalobos, C.; Garcia, H.; Campos-Amezcu, R. Techno-economic feasibility study of small wind turbines in the Valley of Mexico metropolitan area. *Energies* **2019**, *12*, 890. [CrossRef]
178. Orrell, A.; Foster, N.; Morris, S.; Homer, J. 2016 *Distributed Wind Market Report*; Technical Report; Pacific Northwest National Lab. (PNNL): Richland, WA, USA, 2017.
179. Pitteloud, J.D.; Gsänger, S. 2016 *Small Wind World Report*; Technical Report; Pacific Northwest National Lab. (PNNL): Richland, WA, USA, 2016.
180. Small Wind Certification Council. *Xzeres Skystream 3.7 SWCC Summary Report*; Technical Report; Small Wind Certification Council: Brea, CA, USA, 2019.
181. Xzeres. Xzeres SKYSTREAM 3.7 Turbine Specifications. Available online: <https://www.xzeres.com> (accessed on 15 October 2020).
182. Small Wind Certification Council. *Kingspan KW6 SWCC Summary Report*; Technical Report; Small Wind Certification Council: Brea, CA, USA, 2014.
183. Small Wind Certification Council. *Endurance S-343 SWCC Summary Report*; Technical Report; Small Wind Certification Council: Brea, CA, USA, 2014.
184. ENAIR. Aerogenerador ENAIR 200: E200 Manual. Available online: <https://www.enair.es/es/aerogeneradores/e200> (accessed on 15 October 2020).
185. Bergey. Excel 10 Spec Sheet. Available online: <http://www.bergey.com/products/grid-tied-turbines/excel-10/> (accessed on 15 October 2020).
186. Wang, C.N.; Tibo, H.; Duong, D.H. Renewable Energy Utilization Analysis of Highly and Newly Industrialized Countries Using an Undesirable Output Model. *Energies* **2020**, *13*, 2629. [CrossRef]

**Publisher’s Note:** MDPI stays neutral with regard to jurisdictional claims in published maps and institutional affiliations.



© 2020 by the authors. Licensee MDPI, Basel, Switzerland. This article is an open access article distributed under the terms and conditions of the Creative Commons Attribution (CC BY) license (<http://creativecommons.org/licenses/by/4.0/>).